

ME4101B

Mechanical Systems Design

Automation of Manual Regrinding of Gundrill

Final Report

Mentor: Kumar A. Senthil

Group 4

Chain Ming Shan @ Emily Chain (A0202306Y)

Crystal Tan Li Yin (A0202531Y)

Lim Yu Han (A0202230H)

Chung Jun Yu Chester (A0201459J)

Acknowledgement

The team would like to express their thankfulness and appreciation towards National University of Singapore and Halliburton Company for the opportunity to design and work on this project.

The team would like to extend their sincere gratitude to their National University of Singapore Professor Mr. Kumar A. Senthil for his continuous guidance and valuable advice during the project.

The team is very fortunate to have gotten assistance from the staffs at SimTech and National University of Singapore, Mr. Stanley Thian, Dr. Dennis Neo, Dr. Joel Stephen Short, Mr. Lew Maan Tarn, Mr. Lim Soon Cheong and Mr. Tan Choon Huat.

The team would also like to express their deepest thanks to their team-in-charge, Mr. Eldrick Saw and Mr. Terence Toh for their continuous support and assistance in liaising with the company throughout the design project in academic year 2021/2022.

The team is grateful for the approachable staffs from the Halliburton Company such as Mr. Amarjeet Sachan and Mr. Balathandayutham Kathamuthu who clarified the team's doubts whenever needed, providing words of advice and constructive feedback along the way. Finally, the team would like to show their appreciation towards the technician, Mr Li Xiang, for cooperating and sharing his indispensable insights with the team.

Contents

Acknowledgement	ii
List of Figures	vii
List of Tables	xi
Abstract.....	8
Nomenclature	9
1. Introduction	10
1.1 Background.....	10
1.1.1 Partner Company: Halliburton.....	10
1.1.2 Role of Grinding in the Manufacturing Industry	10
1.1.3 Gundrill Regrinding.....	13
1.2 Problem/Solution Statement.....	15
1.3 Objective	16
1.4 Constraints/Customer requirement	17
1.5 Project Management Plan (Gantt Chart)	18
2. Standard Operating Procedure	20
3. Designs/Ideas	21
3.1 Components included in Designs.....	21
3.1.1 Linear Module	21
3.1.2 Vertical Linear Actuator.....	22
3.1.3 Rotary Motor	23
3.2 Enclosed 3 Degree of Freedom (DOF) Design	23
3.3 Open System Design	25
3.4 Multi-Slot Gundrill Support Design	27

3.5	DOF Grinding Wheel Arm Design.....	29
4.	Selection of Final Concept.....	31
4.1	Decision Matrix.....	31
4.2	Modifications and Final Design.....	32
4.3	Revised Final Design	35
4.4	Summary of final idea & pain points of current manual regrinding system.....	38
4.4.1	Increase Accuracy.....	39
4.4.2	Reduce Health Hazard	39
4.4.3	Increase Efficiency	40
4.4.4	Other features	40
5.	Detailed calculations of Final Concept	41
5.1	Assumptions	41
5.2	Known Variables	41
5.3	Set Variables.....	41
5.4	Calculation of Power.....	42
5.5	Calculation of Torque	42
5.6	Calculation of Grinding Force	43
6.	Design of Components	43
6.1	Motor Bracket	43
6.1.1	Initial Design.....	43
6.1.2	First Iteration.....	44
6.1.3	Second Iteration	45
6.2	Gundrill Clamp	47
6.2.1	Initial Design.....	47

6.2.2	First Iteration.....	47
6.3	Spindle	48
6.3.1	Initial Design.....	48
6.3.2	First Iteration.....	49
7.	Simulation	51
7.1	Grinding Wheel Arm Simulation	51
7.1.1	Sub-study 1: Static stress analysis of top portion of grinding wheel arm	52
7.1.2	Sub-study 2: Static-stress analysis of whole grinding wheel arm	54
7.2	Bracket Simulation.....	56
7.2.1	Motor bracket	56
7.2.2	L-bracket for Gundrill Support.....	57
8.	Sourcing of Materials/Components	59
9.	Testing of Concept	68
9.1	Electrical Connections.....	68
9.1.1	Speed control software interface: MEXE02	70
9.2	Components for Testing	71
9.2.1	KUKA KR60 Robotic Arm.....	71
9.2.2	SDR-960-48 Power Supply	73
9.2.3	BLV640NA DC Motor	74
9.2.4	FA-430 Fume Extractor	75
9.3	Physical Assembly.....	76
9.4	Translation of Angles	78
9.5	Program Flow	81
9.6	Testing Criteria	82

9.6.1	Dimensional Accuracy	82
9.6.2	Time Taken	82
9.7	Troubleshooting	83
9.7.1	Reference Axis.....	83
9.7.2	Reference Point.....	83
9.7.3	Parallelism of grinding wheel	84
9.8	Results	85
10.	Discussion.....	87
10.1	Evaluation of Results	87
10.2	Limitations of Design	88
10.3	Recommendations.....	89
11.	Conclusion.....	89
12.	References.....	91

List of Figures

Figure 1: General Trends in the Utilization of Grinding Wheels and Cutting Tools	11
Figure 2: Peripheral Surface Grinding	12
Figure 3: Peripheral Cylindrical Grinding.....	12
Figure 4: Face Surface Grinding.....	13
Figure 5: Face Cylindrical Grinding	13
Figure 6: Dimensions of Gundrill Tip	15
Figure 7: Halliburton Step-By-Step Regrinding Procedure Chart.....	20
Figure 8: Linear Module Working Principle	21
Figure 9: Vertical Linear Actuator Working Principle	22
Figure 10: Rotary Motor Working Principle.....	23
Figure 11: Sketch of Enclosed 3 Degree of Freedom (DOF) Design	24
Figure 12: 3D CAD model of Enclosed 3DOF Design (Front View)	24
Figure 13: 3D CAD model of Enclosed 3DOF (Isometric View)	25
Figure 14: Sketch of Open System Design	26
Figure 15: 3D CAD model of Open System Design (Front View)	26
Figure 16: 3D CAD model of Open System Design (Isometric View).....	27
Figure 17: Sketch of Multi-Slot Gundrill Support Design	28
Figure 18: 3D CAD Model of Multi-Slot Gundrill Support Design (Front View).....	28
Figure 19: 3D CAD Model of Multi-Slot Gundrill Support Design (Isometric View)	29
Figure 20: Sketch of 5DOF Grinding Wheel Arm Design	30
Figure 21: 3D CAD Model of 5DOF Grinding Wheel Arm Design (Front View)	30

Figure 22: 3D CAD Model of 5DOF Grinding Wheel Arm Design (Isometric View)	31
Figure 23: Sketch of Final Design.....	33
Figure 24: 3D CAD Model of Final Design (Front View)	33
Figure 25: 3D CAD model of Final Design (Isometric View)	34
Figure 26: 3D CAD model of Industrial Robotic Arm	36
Figure 27: 3D CAD model of Torque Motor.....	37
Figure 28: 3D CAD Model of Finalised Design (Front View).....	37
Figure 29: 3D CAD Model of Finalised Design (Isometric View)	38
Figure 30: 3D CAD Model of Initial Bracket Design (Isometric View).....	44
Figure 31: 3D CAD Model of 5mm (Top) and 8mm (Bottom) Bracket Design (Isometric View)...	45
Figure 32: 3D CAD Model of Final Bracket Design (Isometric View).....	46
Figure 33: Final Bracket Design	46
Figure 34: 3D CAD Model of Initial Gundrill Clamp Design (Isometric View)	47
Figure 35: 3D CAD Model of Final Gundrill Clamp Design (Isometric View)	48
Figure 36: 3D CAD Model of Initial Spindle Design (Isometric View)	49
Figure 37: 3D CAD Model of Spindle Key (Isometric View).....	49
Figure 38: 3D CAD Model of Final Spindle Design (Isometric View)	50
Figure 39: Final Spindle Design	50
Figure 40: Grinding Wheel Arm Assembly Model for Simulation	51
Figure 41: Mesh Density of Top Portion of Grinding Wheel Arm	53
Figure 42: Von Mises Stress Results for Top Portion of Grinding Wheel Arm	53
Figure 43: Mesh Density of Grinding Wheel Arm Assembly.....	54

Figure 44: Von Mises Stress Results for Grinding Wheel Arm Assembly	55
Figure 45: Joints for Grinding Wheel Arm Assembly	56
Figure 46: Simulation of Motor Bracket	57
Figure 47: Simulation of L-Bracket	57
Figure 48: Driver Configuration.....	69
Figure 49: 15-Pin Configuration	69
Figure 50: Driver Electrical Connections.....	70
Figure 51: PC Display of Motor Software	70
Figure 52: PC Display (Real-Time Motor Status).....	71
Figure 53: Robotic Arm Axis	72
Figure 54: Power Supply.....	73
Figure 55: Motor and Driver.....	74
Figure 56: Fume Extractor	75
Figure 57: Motor Assembly	76
Figure 58: Gundrill Clamp Set-Up.....	77
Figure 59: Full Assembly for Testing.....	77
Figure 60: Tilt on Gundril Clamp (Original).....	78
Figure 61: Tilt on Grinding Wheel (Translated)	79
Figure 62: Swing on Gundrill Clamp	79
Figure 63: Swing on Grinding Wheel	80
Figure 64: Torsion on Gundrill Clamp.....	80
Figure 65: Calibration with Paper.....	84

Figure 66: Checking for Parallelism	85
Figure 67: Display on Keyence Microscope	85
Figure 68: Width of Diamond Band	88

List of Tables

Table 1: Gantt Chart (Semester 1).....	18
Table 2: Gantt Chart (Semester 2).....	19
Table 3: Decision Matrix.....	32
Table 4: Pain Points vs Features	38
Table 5: Bill of Material (Testing of Concept)	59
Table 6: Bill of Material (Actual Implementation)	63
Table 7: Robotic Arm Axis Motion and Speed	72
Table 8: Power Supply Specification	73
Table 9: Motor Specifications.....	74
Table 10: Fume Extractor Specifications	75
Table 11: Measurement of Three Gundrills (in mm) that were manually re-grinded at Halliburton	86
Table 12: Measurements of the Gundrill (in mm) re-grinded by the KR60	86
Table 13: Recorded Time Taken for each trial done on the KR60.....	86

Abstract

The team has been tasked to automate the current manual gundrill regrinding process of the end-user, Halliburton, to reduce health hazards, increase accuracy and efficiency. The current system exposes the technicians to harmful carbide particles and does not have precise methods to measure the accuracy of the regrind in its standard operating procedure (SOP). The inaccuracy of regrind can lead to a higher rate of failure of deep hole drilled products resulting in damage and loss of product. In addition, the process is highly dependent on the skills and experience of the technicians, which varies across different technicians and is therefore inconsistent.

The team's four designs for the automated set-up are the Enclosed 3 Degree of Freedom (DOF) Design, Open System Design, Multi-Slot Gundrill Support Design and 5 DOF Grinding Wheel Mount Design. With many considerations and much feedback from Halliburton, the team's final design of the set-up is an improved version of the 5 DOF Grinding Wheel Mount Design. Calculations and simulations have been carried out on the design model to find areas of high stresses and possibility of failure. Through the simulation results, the team was able to identify the flaws and limitations of the design and revise the design by replacing individual motors with a robotic arm and torque motor.

To carry out testing for proof of concept, the team utilised the KUKA KR60 Robotic Arm in the NUS Advanced Robotics Centre (ARC), and a full assembly which consisted of equipment such as the BLV640NA DC Motor drive the grinding wheel, a 48V DC power supply to drive the motor and a gundrill clamp to hold the gundrill in place. Calibration and troubleshooting were carried out on the robotic arm according to the required programme flow for automated regrinding, and a total of three tests were conducted to ascertain the effectiveness of the automated process. The results of the tests were studied and evaluated, whereby the $\frac{1}{4}$ diameter on the gundrill was the main parameter used to determine the accuracy of the regrind, and time taken was another factor used to consider the speed of the automated process.

Nomenclature

ω	Angular speed (rad/s)
N	Rotational speed (RPM)
v	Linear velocity (m/s)
v_c	Cutting speed (m/s)
f	Feed rate of grinding (m/s)
r	Radius of grinding wheel (m)
D	Diameter of cutting tool (m)
d	Depth of cut (m)
b	Width of cut (m)
F_{grinding}	Total grinding force (N)
$F_{\text{grinding(SF)}}$	Total grinding force with safety factor (N)
P	Power requirement for motor (W)
T	Torque (Nm)
T_{SF}	Torque with safety factor (Nm)
u	Specific grinding energy for Tungsten Carbide (J/m ³)
MRR	Material removal rate (m ³ /s)

1. Introduction

This report highlights the team's progress and design-thinking process throughout the project, various ideas and concept testing of the chosen idea.

1.1 Background

1.1.1 Partner Company: Halliburton

Halliburton is one of the largest energy product and services providers worldwide. First established in 1919, Halliburton collaborated and served many national, independent, and major oil and gas companies around the world. Halliburton provides services from managing geological data, drill, and formation evaluation, locating hydrocarbons, and optimizing production throughout the life of the asset [1]. The Completion Technology and Manufacturing Centre was opened by Halliburton in 2013 and is equipped with the full set of Completion Tools products becoming one of its key product service lines. Test facilities and laboratories are also available at the manufacturing centre which conducts complex processes, which includes small deep-hole gun drilling, high-alloy material precision machining and electrode discharge machines [2].

1.1.2 Role of Grinding in the Manufacturing Industry

Dating back more than 2 centuries ago, the utilization of abrasives for shaping became prominent. Abrasives were used to shape and cut stones and rocks for constructing buildings and edifices, such as the famous Pyramids of Giza located in Egypt, one of the modern marvels in present day. In fact, abrasives are continually relied on in growingly diverse applications in the manufacturing industry. Even in the distant past, grinding was recognized as an effective finishing process for products that were reaching the most valuable stage in the production.

Grinding evolved into a metal manufacturing process around the nineteenth century [3] and had a significant role in the production of tools, microelectronic devices, and engines. Some of these engines are commonplace in the present-time, including the steam engines, internal combustion engines and jet engines. Grinding refers to a term used in modern manufacturing practice to illustrate machining with high-speed abrasive wheels, belts, and pads [4].

Late in the twentieth century, grinding was acknowledged as a strategic procedure for high-technology applications. These applications include the manufacturing of missile guidance

systems and aircraft engines, and the fabrication of optical quality surfaces for electronic and communications devices. To further understand why grinding remains a highly effective and strategic process in the manufacturing industry, it is essential to scrutinize the different benefits of grinding.

Grinding brings about low costs, great quality and high speed of production in the manufacturing industry. It is seen as the cheapest and least sophisticated process for machining hard materials and is capable of achieving the required quality and speed of production together with process reliability [5], beating out many other alternative processes in the industry including hard turning. High accuracy can be attained through grinding and close tolerances can be accounted for in terms of surface texture, shape, and size. Serving as a versatile process in the manufacturing industry, grinding can be used to machine both large and small parts. For instance, large parts such as tool slideways whereby straightness is a strict criterion to be followed and tolerances are in the degree of microns, can be machined through grinding. Conversely, small parts including silicon wafers where tolerances range from micron to submicron, can also be machined through grinding.

In recent years, grinding has transitioned into a process capable of producing very high-quality parts and for fast economic output [6]. This is depicted in Figure 1 where cutting tools and grinding are perceived to be rising in competitiveness for both machining accuracy and production rate, whereby production rate is dependent on material removal rate.

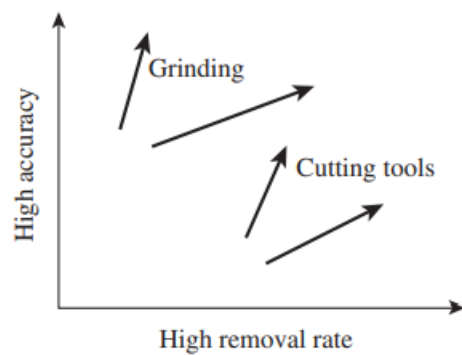


Figure 1: General Trends in the Utilization of Grinding Wheels and Cutting Tools

There are two main classes of grinding, which is the flat surface grinding and cylindrical grinding. The four basic grinding processes branch out of these two main classes, and they refer to peripheral surface grinding, peripheral cylindrical grinding, face surface grinding and face cylindrical grinding. Surface grinding is usually performed on flat surfaces to produce a smooth finish while cylindrical grinding is commonly used for precision grinding of end faces, outer and conical surfaces [7].

Peripheral surface grinding is a process whereby the periphery (flat edge) of the wheel comes into contact with the workpiece and produces a flat surface.

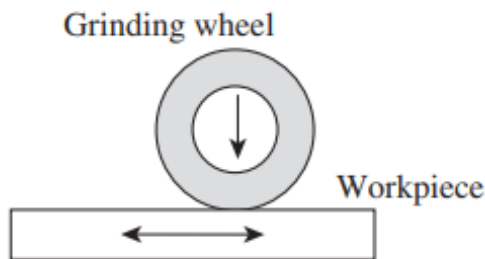


Figure 2: Peripheral Surface Grinding

Peripheral cylindrical grinding is a process whereby the periphery (flat edge) of the grinding wheel comes into contact with the workpiece and produces a rounded surface.

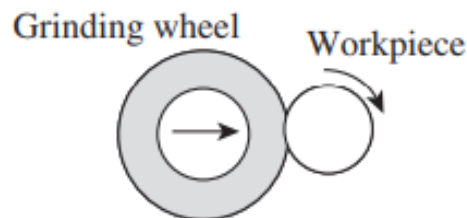


Figure 3: Peripheral Cylindrical Grinding

Face surface grinding is a process whereby the flat surface of the grinding wheel comes into contact with the workpiece and produces a flat surface. For gundrill regrinding, face surface grinding is the main method utilised.

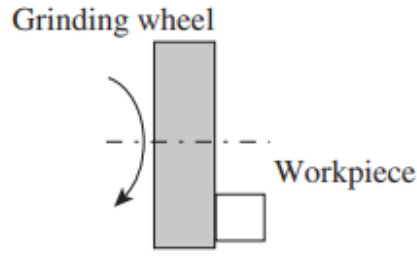


Figure 4: Face Surface Grinding

Face cylindrical grinding is a process whereby the flat surface of the grinding wheel comes into contact with the workpiece and produces a rounded surface.

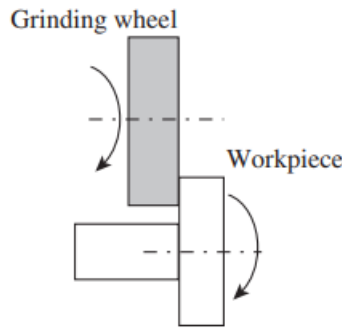


Figure 5: Face Cylindrical Grinding

1.1.3 Gundrill Regrinding

Gundrilling is a self-piloting drilling process that uses long and thin cutting tools, usually of diameter 1 to 50mm to generate deep, straight, and precise-diameter holes in a workpiece at high depth-to-diameter ratios. By using pressurized coolant for chip cleaning even at extreme depths, the gundrilling process can drill deep holes, far beyond what is achievable with conventional machining methods and tooling [8]. Gundrills are differentiated from standard twist drills by its unique head geometry. A gundrill only has one effective cutting edge to perform the cutting action and one or two flutes to remove chips, whereas a twist drill has two cutting edges and two flutes that enables chip removal as it travels through the workpiece [9].

For industries like aerospace, automotive, oil, medical as well as military, gundrilling of high-aspect-ratio holes is extremely crucial as it can create highly precise features for high-yield-

strength superalloys such as Monel, Titanium, and Inconel [10]. Gundrilling was primarily developed to produce gun barrels, where both straightness and barrel lifespan were critical to ensure proper barrel operations. Since then, the gundrilling method and tools have been optimised for maximum performance and use on modern, specialized machinery [8].

There are two configurations of gundrill, namely solid carbide gundrills and indexable carbide gundrills. Due to a reduction in torsional vibration and greater rigidity, solid carbide gundrills have a longer tool life and provides better performance and process reliability. Indexable carbide gundrills, on the other hand, have increased tool life owing to its indexable design, edge treatment and complete coating. These gundrills also allow quick replacement of worn parts, reducing downtime and improving versatility [9]. Gundrills, just like any other tool, will wear out after extended usage. Resharpening or regrinding is then required for gundrills usually after drilling about 25.4m and regardless of the technician's expertise level, drilling holes with a blunt gundrill will compromise hole accuracy and finishing [11]. Furthermore, a dull cutting edge will cause chips produced to be uneven and more thrust and torque will be required to drill the hole. This can lead to increased drifts, more runoffs, and spikes in the coolant pressure, resulting in failure [11]. During the regrinding process, the blunt surface will be ground off to reveal the raw carbide beneath. Coated and uncoated carbide tips can both be resharpened without affecting the performance and each gundrill can be regrinded up to 8 to 10 times before the tip length becomes unusable [12]. Regrinding of solid carbide gundrill tips will be the sole focus of this report.

A grinding system is necessary to begin the regrinding process, which includes a grinder, gundrill support and equipment for calibrating and inspecting the tip of the drill. Companies can opt to perform the regrinding process in their workshop or have it resharpened by the original equipment manufacturer (OEM) [12]. A slight variation in gundrill tip geometry can have detrimental consequences on the final workpiece, adversely affecting the roundness, straightness and depth of hole, size control, finishing and cylindricity. As a result, technicians will have to change out tools more frequently and limit feed rate to obtain the desired tolerances [11]. Once the regrinding process is completed, the carbide tip will be inspected using a digital

camera, allowing technicians to take measurements and detect faults without having to remove the gundrill from the support.

1.2 Problem/Solution Statement

The existing manual regrinding process poses significant health risks to the technicians as carbide particles are released during the regrinding process. These carbide particles are detrimental to health and can induce wheezing, coughing and shortness of breath when inhaled. Repeated exposure may also cause scarring of lung tissues and impair lung function. Following the completion of the regrinding process, the dimensions of the gundrill taper ($\frac{1}{4}$ diameter) as shown in Figure 6, are estimated using the vernier calliper and micrometre screw gauge.

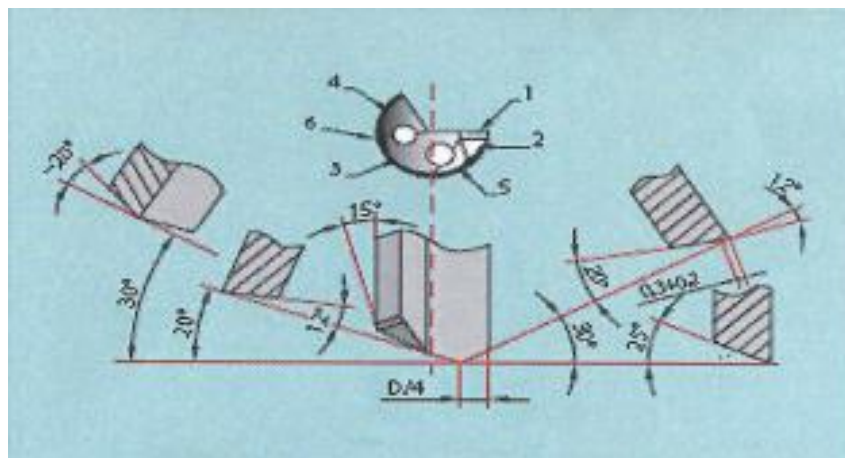


Figure 6: Dimensions of Gundrill Tip

The absence of instruments and applications for precise measurements compromises the accuracy of the dimensions, resulting in inconsistencies. This affects the diameter of the drilled hole and causes unnecessary taper. Furthermore, the company aims to enhance efficiency to cut down on human resources and costs. As the time required for the manual regrinding process is heavily dependent on the technician's experience, it varies among technicians. Therefore, the use of automation allows for consistent regrinding duration and quality regardless of experience level.

1.3 Objective

The main objective of the project is to automate the regrinding process of carbide tips for gundrills to increase accuracy and efficiency of the process, while keeping it safe for the technicians.

In high-speed regrinding process, carbide particles are produced and released into the surroundings. Due to its minute size, these airborne carbide particles can be inhaled by technicians without them noticing. This is a major health concern as these carbide particles are extremely detrimental to human's health. According to experts, the airborne carbide particles can tear up the lung tissue which can damage the organ in a long run [13]. As a result, technicians are required to equip themselves with personal protective equipment (PPE) such as goggles, N95 mask and gloves during the regrinding process. Furthermore, an industrial graded vacuum is installed near the grinding wheel to remove the dust particles.

The finishing and quality of the gundrill is heavily dependent on the technicians' skill and experience level. Factors such as brightness of the polished surface and taper dimension are controlled by the technicians' judgement. As a result, this can lead to inconsistencies in the final dimension among different technicians. Inaccuracies in gundrill will affect the dimension of the deep drilled product, increasing the taper of the drilled hole. To ensure that the taper is still within range, technicians must perform checks after each drill of a certain depth, which depends on the material of the deep drilled product. If the taper is found to be out of range, the deep drilled product must be discarded and remade leading to huge product and financial losses in the company. Hence, it is necessary for the company to reduce the rate of failure due to regrinding inaccuracies. With automation, gundrills can be more accurate, consistent and of higher quality, thus reducing the failure rate.

According to the information and data that the team has collected from Halliburton technicians, an experienced technician would take about 10 minutes to complete the gundrill regrinding process. On the other hand, less experienced or new technicians can take up to 15 minutes. The automation of this process would allow this duration to be consistent regardless of the experience of technicians. In addition, manpower is only required for the loading and unloading

of gundrill into the machine, hence freeing up the technician during the regrinding process. This would allow the technicians to work on other tasks, thereby increasing efficiency.

1.4 Constraints/Customer requirement

The project and design have two major conditions that must be met: space constraint and dimensional tolerance. For the design to be executed, the working area must fit within the available floor space at Halliburton. The measured floor space at Halliburton is 2.08 x 2.94 m. The working area includes the area for technicians to walk around, the tabletop area and the extra space needed for the entire length of the gundrill. The required dimensional tolerance of 51 microns was given as an important criterion to the team by Halliburton. For this project, dimensional tolerance is determined by the tolerance of motors/robotic arms used, which would bring the total cost higher.

1.5 Project Management Plan (Gantt Chart)

The timeline followed by the team in Semester 1 is as shown in Table 1 and the timeline followed in Semester 2 is shown in Table 2.

Table 1: Gantt Chart (Semester 1)

Task	Duration	Start time	End time	Target	Week 0 (02/08/21 - 08/08/21)	Week 1 (09/08/21 - 15/08/21)	Week 2 (16/08/21 - 22/08/21)	Week 3 (23/08/21 - 29/08/21)	Week 4 (30/08/21 - 05/09/21)	Week 5 (06/09/21 - 12/09/21)	Week 6 (13/09/21 - 19/09/21)	Recess (20/09/21 - 26/09/21)	Week 7 (27/09/21 - 03/10/21)	Week 8 (04/10/21 - 10/10/21)	Week 9 (11/10/21 - 17/10/21)	Week 10 (18/10/21 - 24/10/21)	Week 11 (25/10/21 - 31/10/21)	Week 12 (01/11/21 - 07/11/21)	Week 13 (08/11/21 - 14/11/21)	Reading (15/11/21 - 21/11/21)	Exam (22/11/21 - 28/11/21)	Semester Break (09/11/21 - 09/01/22)
Halliburton Site Visit	1 Day	02/08/21	08/08/21	Planned																		
NUS Gundrill Lab Visit	1 Day	02/08/21	08/08/21	Actual																		
Brain Storming/Generation of Ideas	1 Week	09/08/21	15/08/21	Planned																		
Writing of Proposal	1 Week	16/08/21	22/08/21	Actual																		
Submission of Proposal to Halliburton	1 Week	23/08/21	29/08/21	Planned																		
Creation of 3D CAD Model of Ideas	1 Week	23/08/21	29/08/21	Actual																		
Presentation of idea to Halliburton	1 Day	06/09/21	12/09/21	Planned																		
Getting Feedback from Halliburton on Design Concept	1 Week	06/09/21	12/09/21	Actual																		
Approval and Finalization of design concept from Halliburton	1 Week	20/09/21	26/09/21	Planned																		
Finalized sketch of chosen design	1 Week	28/09/21	03/10/21	Planned																		
Creating CAD models for chosen design	3 Week	27/09/21	17/10/21	Actual																		
Start Detailed Analysis/Calculations	3 Week	27/09/21	17/10/21	Planned																		
Simulation	1 Week	18/10/21	24/10/21	Actual																		
Source for actual components / materials for fabrication and get quotations	4 Week	27/09/21	24/10/21	Planned																		
Get Quotation for actual components / materials	2 Week	25/10/21	07/11/21	Actual																		
Interim Report and Presentation (for NUS)	1 Day	08/11/21	14/11/21	Planned																		
Create Bill of Material (BOM)	1 Week	08/11/21	14/11/21	Actual																		
Order Components	5 Weeks	06/12/21	09/01/22	Planned																		
				Actual																		

Table 2: Gantt Chart (Semester 2)

Task	Duration	Start time	End time	Target	AY 21/22 Semester Break (06/11/21 - 09/01/22)	AY 21/22 S2 Week 1 (10/01/22 - 16/01/22)	AY 21/22 S2 Week 2 (17/01/22 - 23/01/22)	AY 21/22 S2 Week 3 (24/01/22 - 30/01/22)	AY 21/22 S2 Week 4 (31/01/22 - 06/02/22)	AY 21/22 S2 Week 5 (07/02/22 - 13/02/22)	AY 21/22 S2 Week 6 (14/02/22 - 20/02/22)	AY 21/22 S2 Recess (21/02/22 - 27/02/22)	AY 21/22 S2 Week 7 (28/02/22 - 06/03/23)	AY 21/22 S2 Week 8 (07/03/22 - 13/03/22)	AY 21/22 S2 Week 9 (14/03/22 - 20/03/22)	AY 21/22 S2 Week 10 (21/03/22 - 27/03/22)	AY 21/22 S2 Week 11 (28/03/22 - 03/04/22)	AY 21/22 S2 Week 12 (04/04/21 - 10/04/22)	AY 21/22 S2 Week 13 (11/04/22 - 17/04/22)
					Planned	Actual	Planned	Actual	Planned	Actual	Planned	Actual	Planned	Actual	Planned	Actual	Planned	Actual	
Design/Review Components (Brackets/Spindle/etc)	5 Weeks	06/12/21	09/01/22																
3D Print designed components	5 Weeks	06/12/21	09/01/22																
Send out components for fabrication	5 Weeks	06/12/21	09/01/22																
Order Components	5 Weeks	06/12/21	09/01/22																
Perform Demo (at Hiwin)	1 Day	23/12/21	23/12/21																
Risk Assessment	2 Weeks	17/01/22	30/01/22	Planned															
Fabricate Spindle at NUS	1 Weeks	24/01/22	30/01/22	Planned															
Receive Ordered Components	2 Weeks	24/01/22	06/02/22	Planned															
Receive Fabricated Components	2 Weeks	14/02/22	27/02/22	Planned															
Programming	1 Weeks	28/02/22	06/03/22	Planned															
Perform Testing	1 Weeks	07/03/22	13/03/22	Planned															
Troubleshooting (ARC Lab)	2 Weeks	14/03/22	27/03/22	Planned															
Final Slides	2 Weeks	28/03/22	08/04/22	Planned															
Final Report	2 Weeks	28/03/22	08/04/22	Planned															
Final Presentation	1 Day	13/04/22	13/04/22	Planned															
				Actual															

2. Standard Operating Procedure

The current manual regrinding procedure carried out by the technicians is illustrated in the chart below. For the regrinding process, the technicians will perform the six steps in sequence. For the first step, the technician will adjust the swing angle to -30° , the tilt angle to $+12^\circ$ and the torsion angle within the range of $+5^\circ$ to $+10^\circ$. The technician will then perform the other steps according to the chart to complete the manual regrinding process.

5		 	Swing	Tilt	Torsion	Measure		
			-30	+12	+5 .. 10	$> \frac{D}{4}$		
Adjust Torsion so that in OP2 the chamfer runs parallel to D/2								
6		 	Swing	Tilt	Torsion	Measure		
			-30	+20	+5 .. 10	0.3 to 0.5 mm		
Width of chamfer equal to guide chamfer								
7		 	Swing	Tilt	Torsion	Measure		
			+20	+12	-5	$\frac{D}{4}$		
8		 	Swing	Tilt	Torsion	Measure		
			+30	+12	+55			
9		 	Swing	Tilt	Torsion	Measure		
			0	+25	0			
10		 	Swing	Tilt	Torsion	Measure		
			+75					
Twist the drill at the circumference without damaging the cutting edges.								
If in doubt, please check with your team lead, stop work and inform supervisor if issues not resolved								
 COMPARATOR								

Figure 7: Halliburton Step-By-Step Regrinding Procedure Chart

3. Designs/Ideas

The team came up with 4 designs of the automated gundrill regrinding machine. In the designs which the team has come up with, the technicians are first required to place and clamp the gundrill onto the gundrill support manually. Next, the technicians will input user-defined values on the display interface and start the automation process. Once the automation begins, the technician will be freed up for other tasks. To summarise, manpower is only required at the start and the end of the grinding process. The working principles of each design will be elaborated in the following sections. Before the various designs are explained, the components that make up the designs will be elaborated in detail.

3.1 Components included in Designs

3.1.1 Linear Module

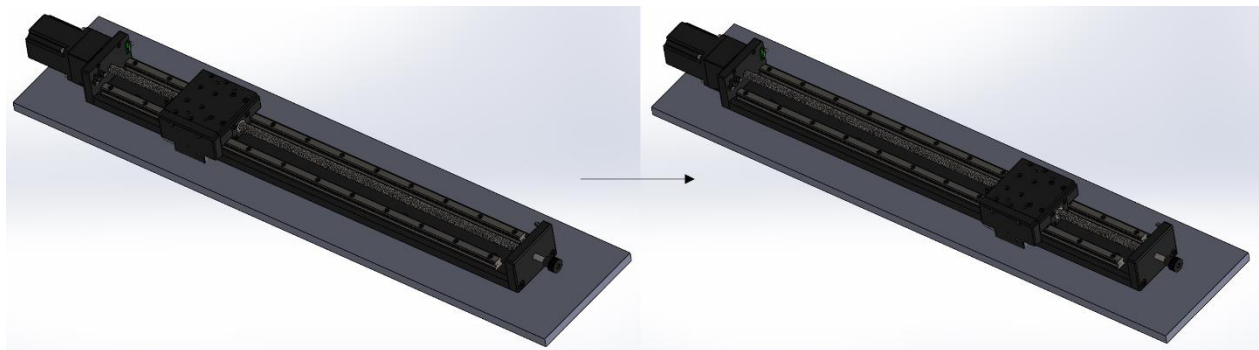


Figure 8: Linear Module Working Principle

Consisting of a lead screw and a linear guide, the linear module is a mechanical structure that provides linear motion [14]. As seen in the figure above, the linear module is used with a power motor and can be utilized to automatically reciprocate a workpiece. For the team's designs, the linear module will be used mainly for translational movement in the horizontal axes.

3.1.2 Vertical Linear Actuator

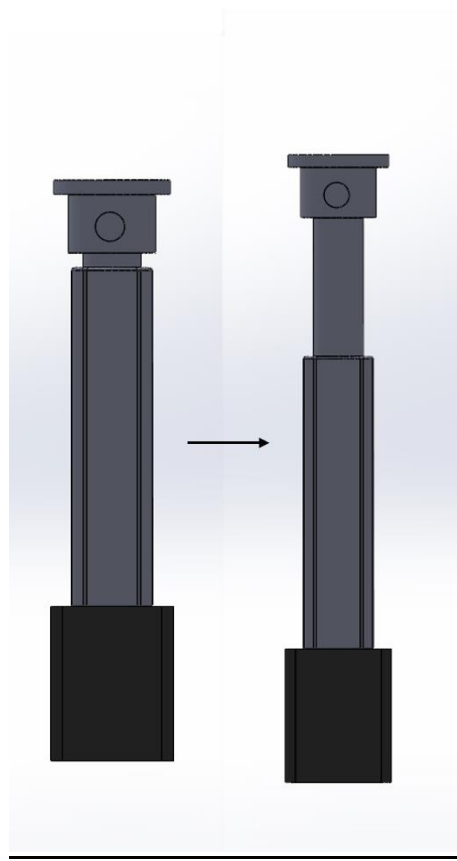


Figure 9: Vertical Linear Actuator Working Principle

Similar to the linear module described earlier, a vertical linear actuator provides linear motion. An actuator is a device that requires an energy source input and an external signal input. It converts the rotational motion of an AC motor into linear motion and can provide both push and pull movements [15], as shown in the figure above. For the team's designs, the vertical linear actuator will be used mainly for translational movement in the vertical axis, either in the grinding wheel arm or the gundrill support arm.

3.1.3 Rotary Motor

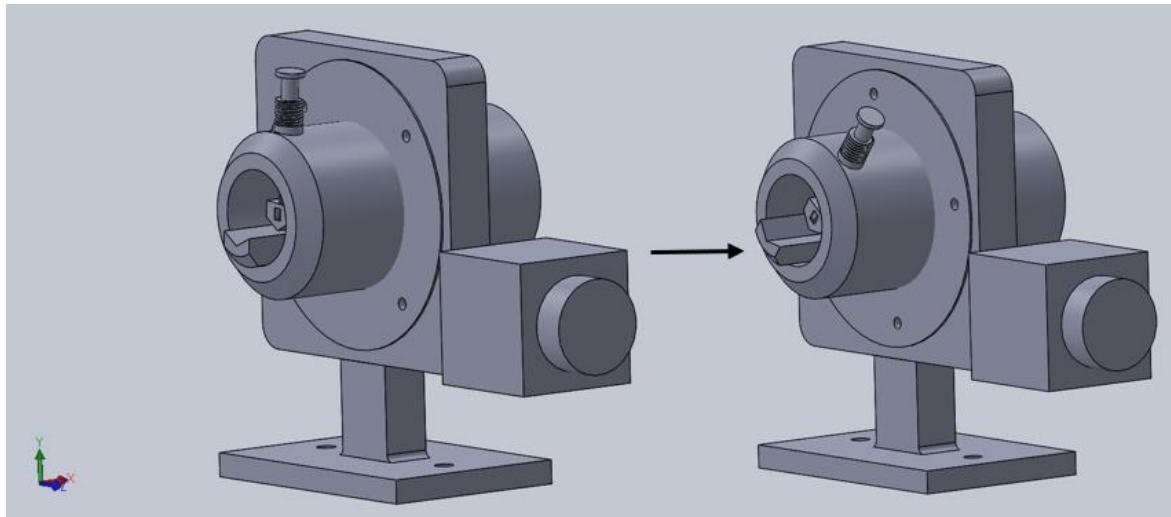


Figure 10: Rotary Motor Working Principle

A rotary motor will enable rotation about the x-axis, rotating the entire gundrill clamp. Driven by a bevel gear system, the rotary motor mounted on the side of the clamp will transfer its motion to the gundrill clamp, which lies at a 90° angle perpendicular to the shaft of the rotary motor. Hence, as seen in Figure 10, the gundrill clamp rotates about the x-axis.

3.2 Enclosed 3 Degree of Freedom (DOF) Design

The figures below illustrate the overall look of this design and the axes convention that is utilized. This design consists of a grinding wheel arm and gundrill support, each with three degrees of freedom. The grinding wheel arm will rotate about the y and z-axes and translate in the y-axis. The grinding wheel will also spin, rotating about the x-axis. On the right, the gundrill support will rotate in the x-axis and translate in the x and z-axes. The entire system will be enclosed in a transparent casing with an industrial grade vacuum attached. Around the cut-out on the casing for the gundrill, a rubber seal is used to maintain airtightness, preventing carbide particles from escaping. An additional moveable support will also be introduced to prevent longer gundrills from sagging and vibrating. There will also be a display interface to allow for input of user-defined variables. Disadvantages of this design include requiring a greater amount of space to accommodate for the movement of the gundrill and its additional support as well as having more moving parts, causing more wear.

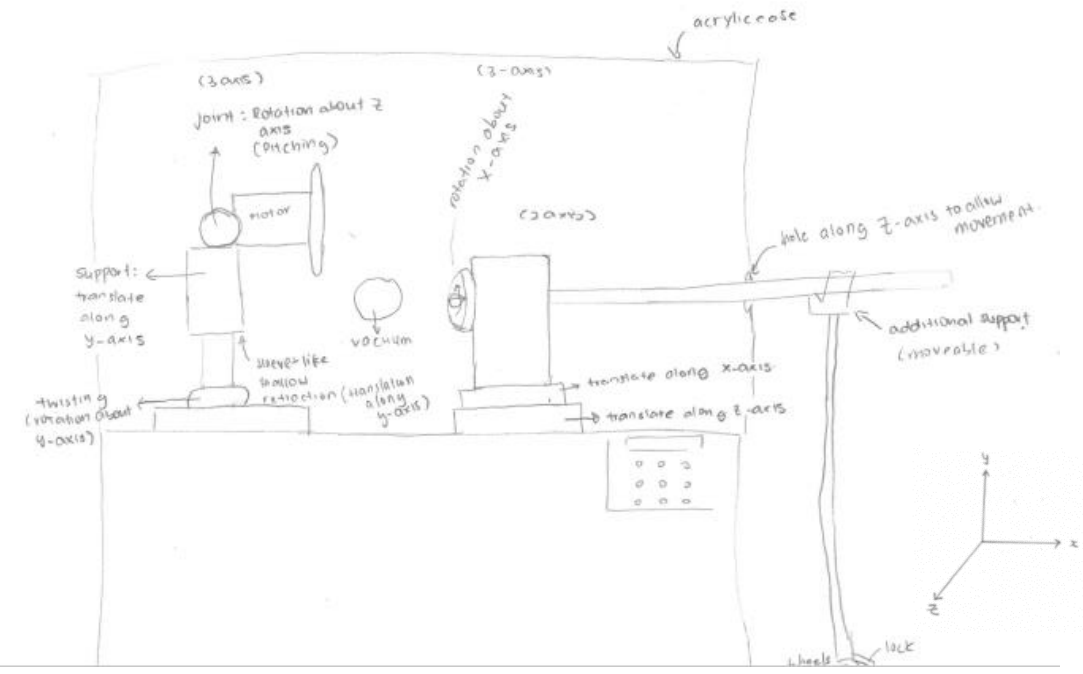


Figure 11: Sketch of Enclosed 3 Degree of Freedom (DOF) Design

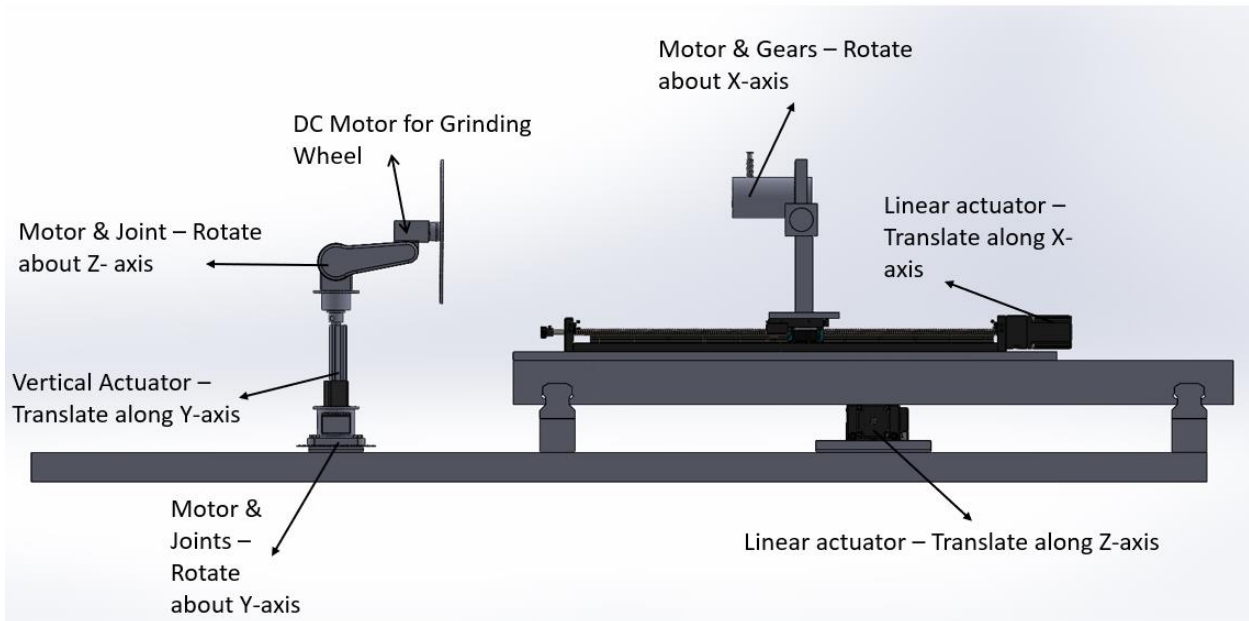


Figure 12: 3D CAD model of Enclosed 3DOF Design (Front View)

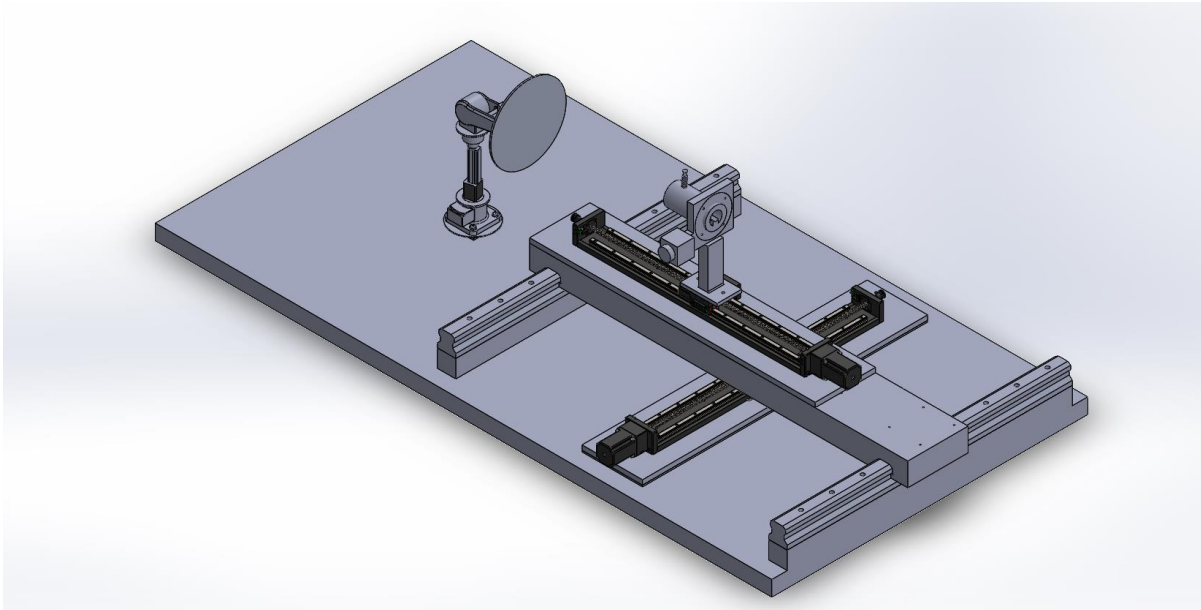


Figure 13: 3D CAD model of Enclosed 3DOF (Isometric View)

3.3 Open System Design

The figures below show the second design and its axes convention. This design comprises a grinding wheel arm that is solely responsible for translating movements in the 3 axes and a gundrill support that is responsible for the rotational motions in the 3 axes. In this design, the original configuration of Halliburton's manual regrinding machine is retained, making it the most straightforward among the ideas. Similar to the enclosed 3 DOF design mentioned in the previous section, it will have a display interface and an industrial grade vacuum. Due to the rotation of the gundrill support about the z-axis, it is not feasible to enclose the entire system, and may result in the presence of carbide particles in the environment. The swinging of the gundrill's tail end can also potentially cause injuries to personnel or damage the gundrill and equipment. As it is impractical to introduce additional supports, sagging and vibration will occur due to the excessive movement of the gundrill.

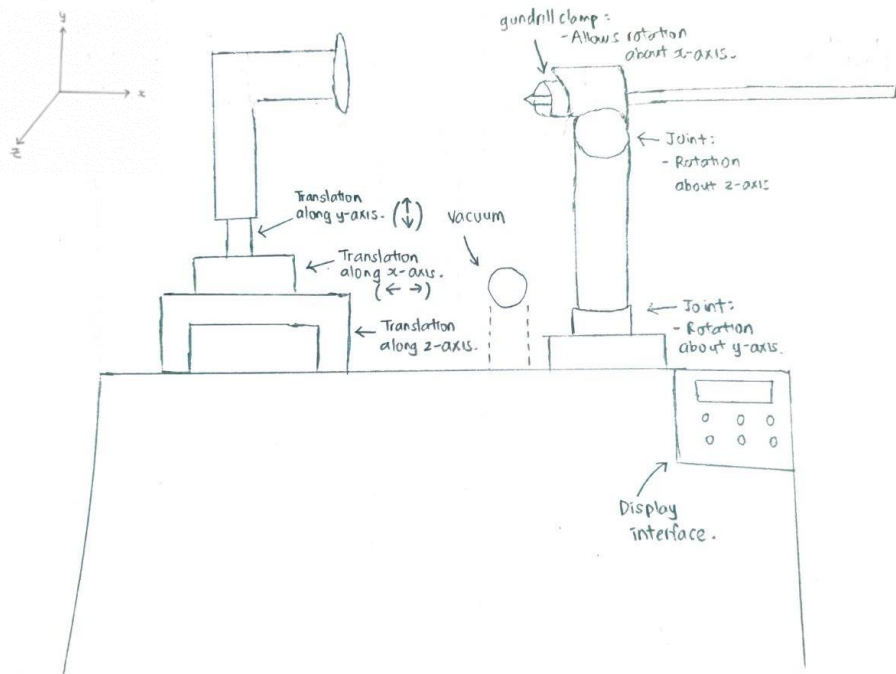


Figure 14: Sketch of Open System Design

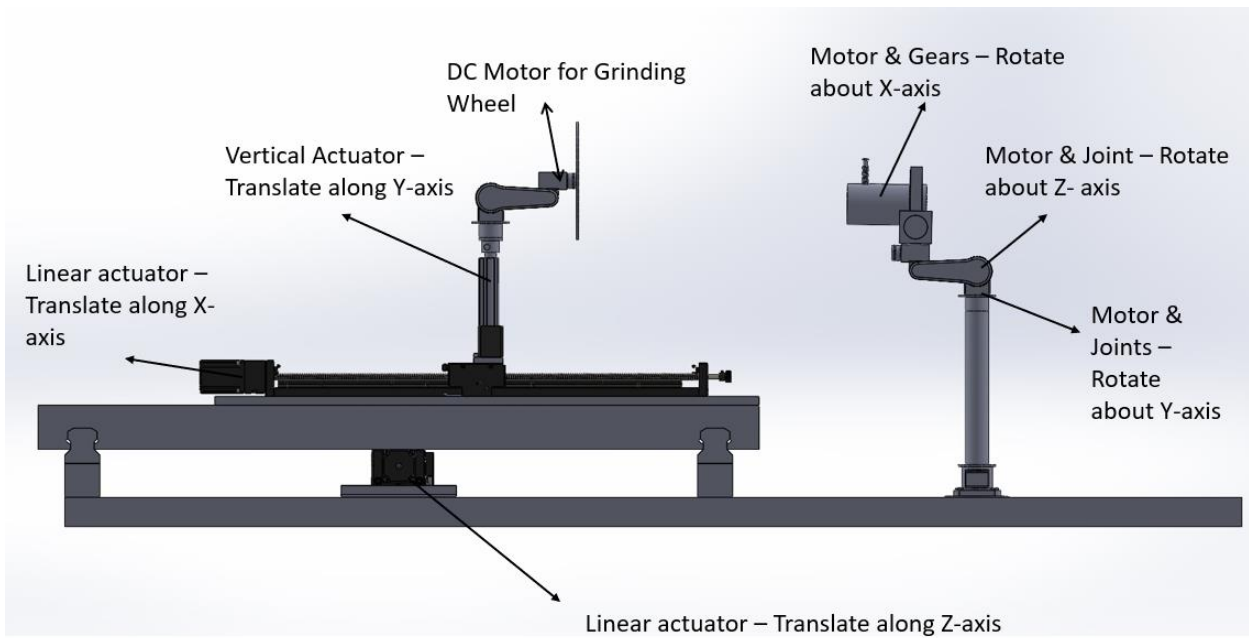


Figure 15: 3D CAD model of Open System Design (Front View)

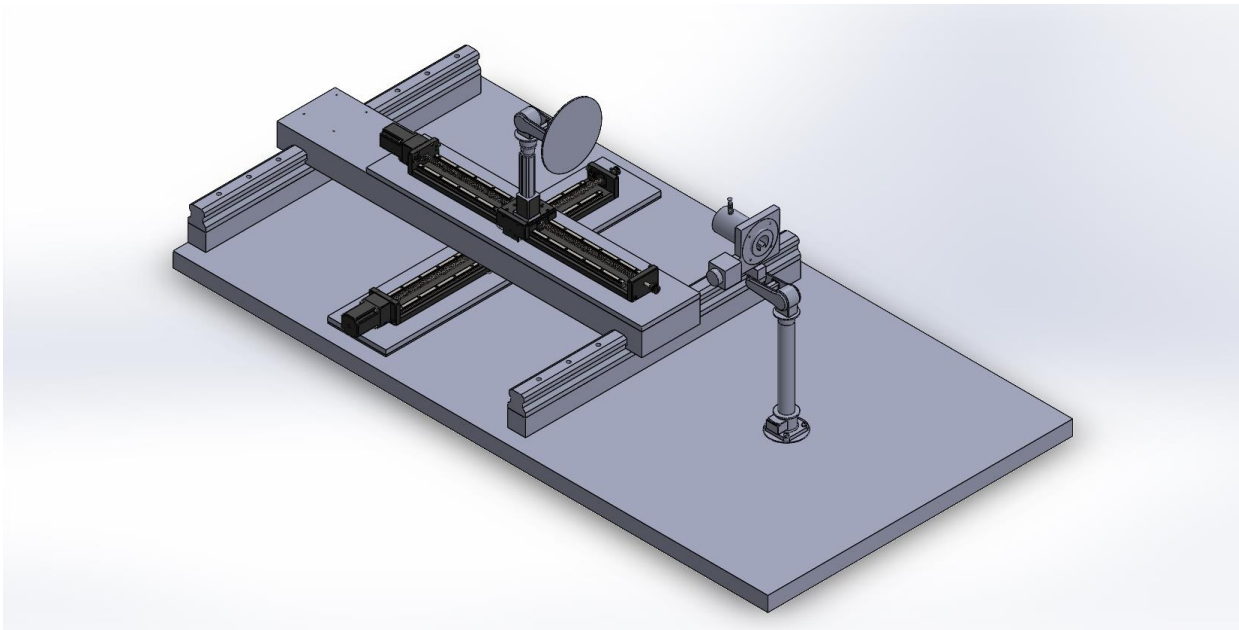


Figure 16: 3D CAD model of Open System Design (Isometric View)

3.4 Multi-Slot Gundrill Support Design

The figures below show the team's third design and axes convention. The highlight of this design is the multi-slot gundrill support which allows 4 gundrills to be worked on simultaneously. The support is kept stationary and the clamp for each gundrill will be able to rotate in the x-axis. The grinding wheel arm will be able to translate in all 3 axes and rotate in the y-axis. The entire system will be enclosed in a transparent casing with a rubber seal around the hole entrance for the gundrills to improve the airtightness. Like the other designs, this design also comes with an industrial grade vacuum and display interface. The syncing of the 4 rotating clamps can be challenging in the implementation of this design. The team deems this solution as unsuitable and inefficient for Halliburton as the company does not specialize in regrinding carbide tips of gundrills only. At Halliburton, only a single gundrill is used during the drilling process. Once the carbide tip is worn out, the same drill is resharpened several times until the length of the solid carbide tip becomes insignificant.

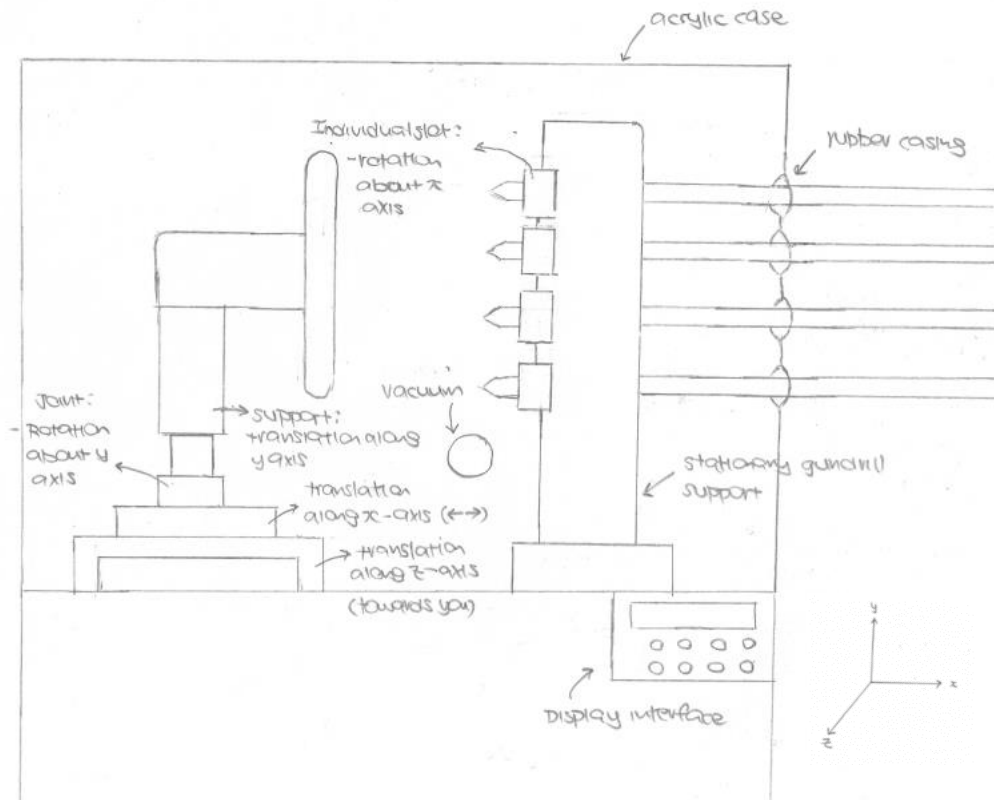


Figure 17: Sketch of Multi-Slot Gundrill Support Design

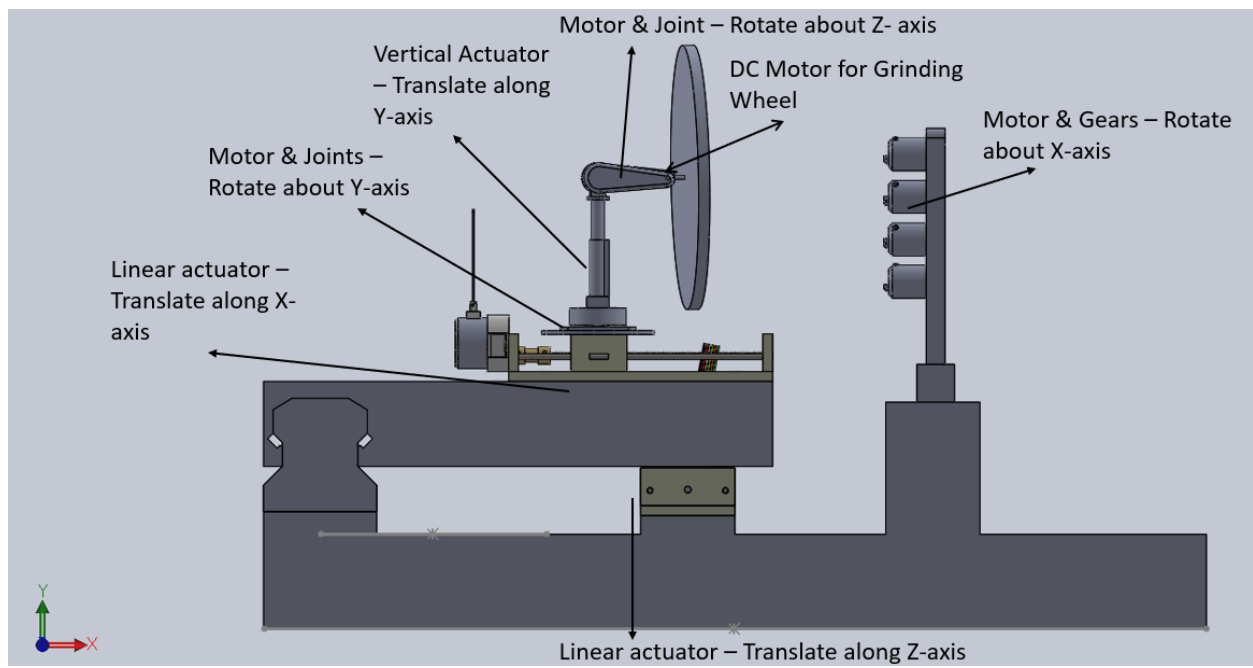


Figure 18: 3D CAD Model of Multi-Slot Gundrill Support Design (Front View)

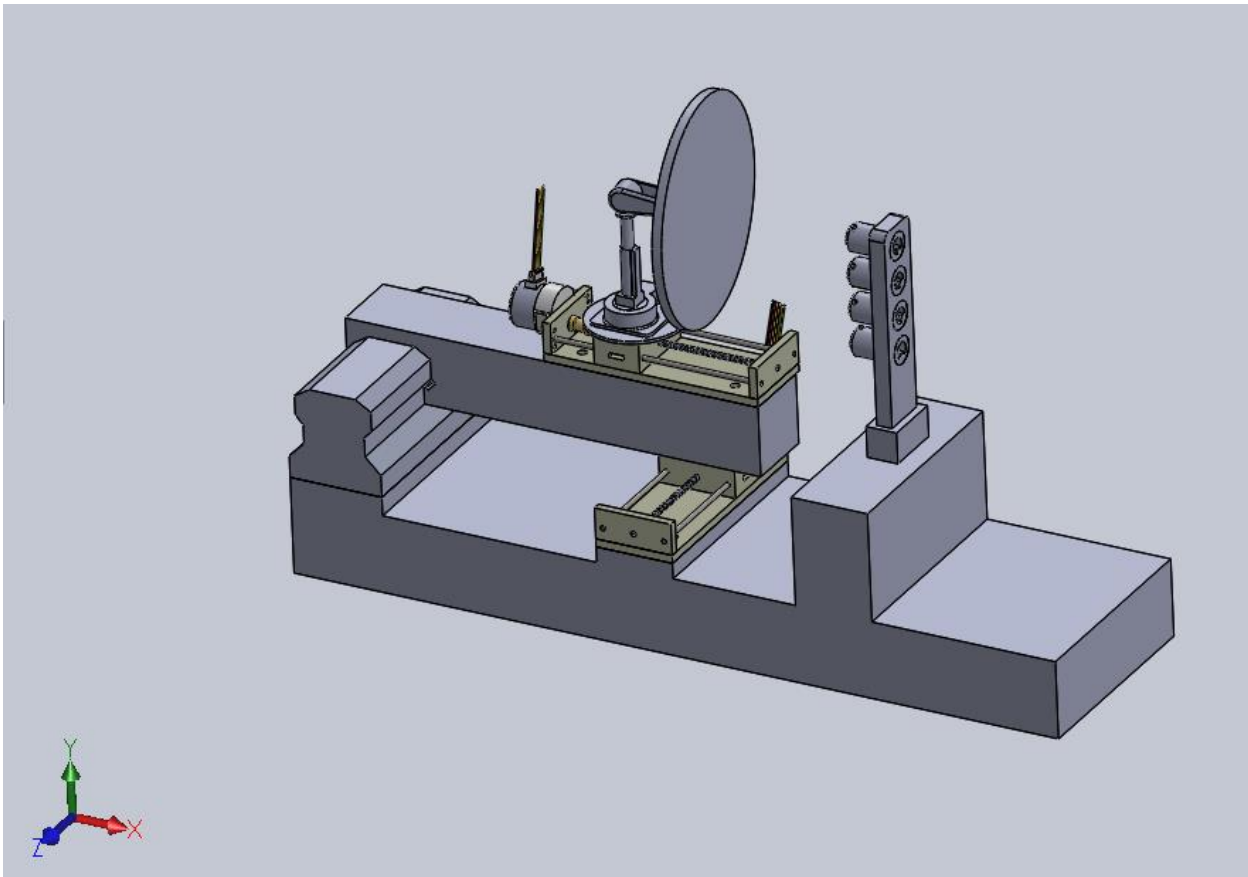


Figure 19: 3D CAD Model of Multi-Slot Gundrill Support Design (Isometric View)

3.5 DOF Grinding Wheel Arm Design

The figures below show the last design and its axes convention. This design depends heavily on the movement of the grinding wheel. Similar to the other ideas, this design has an industrial vacuum, transparent casing and display interface. The grinding wheel arm in this design is responsible for the translating motion in the x, y and z-axes as well as the rotating motion in the y and z-axes. A grinding wheel and motor will be attached at the top of the arm which will rotate in the x-axis. On the other hand, the gundrill support will be fixed to the table set up and it will contain a clamp that rotates in the x-axis. An additional support will also be added for longer gundrills to prevent vibration and sagging. The advantage of this design is that it requires lesser amount of space and setup is easy to enclose as the gundrill will only be rotating in one axis and will not be making large swinging movements.

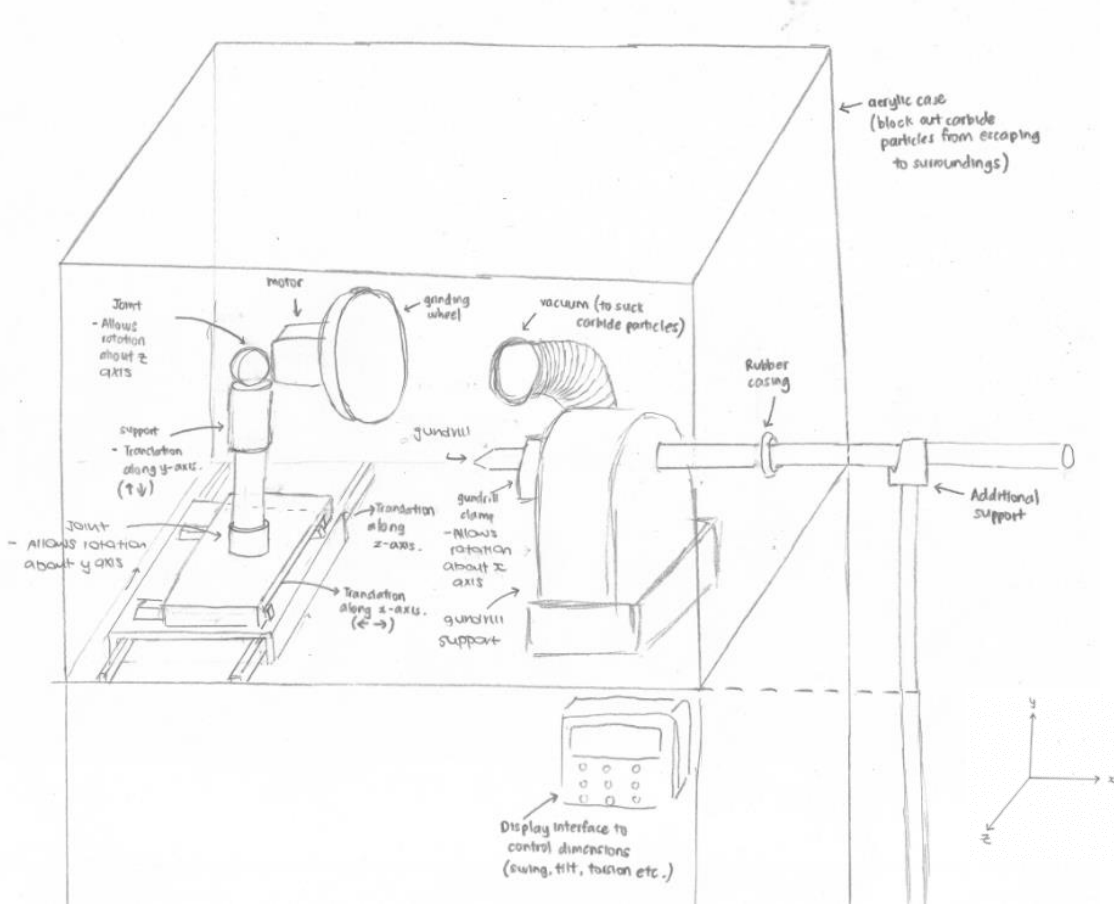


Figure 20: Sketch of 5DOF Grinding Wheel Arm Design

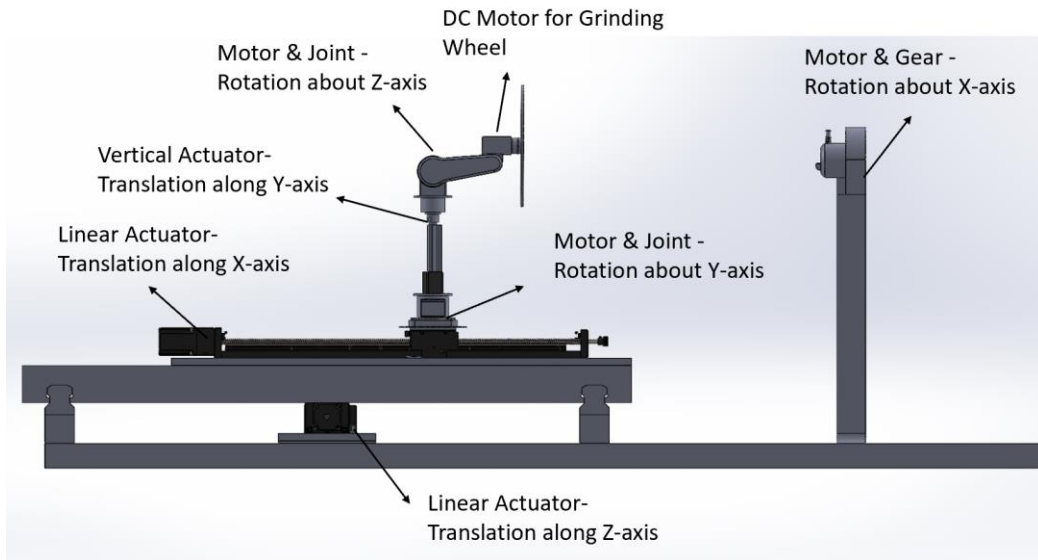


Figure 21: 3D CAD Model of 5DOF Grinding Wheel Arm Design (Front View)

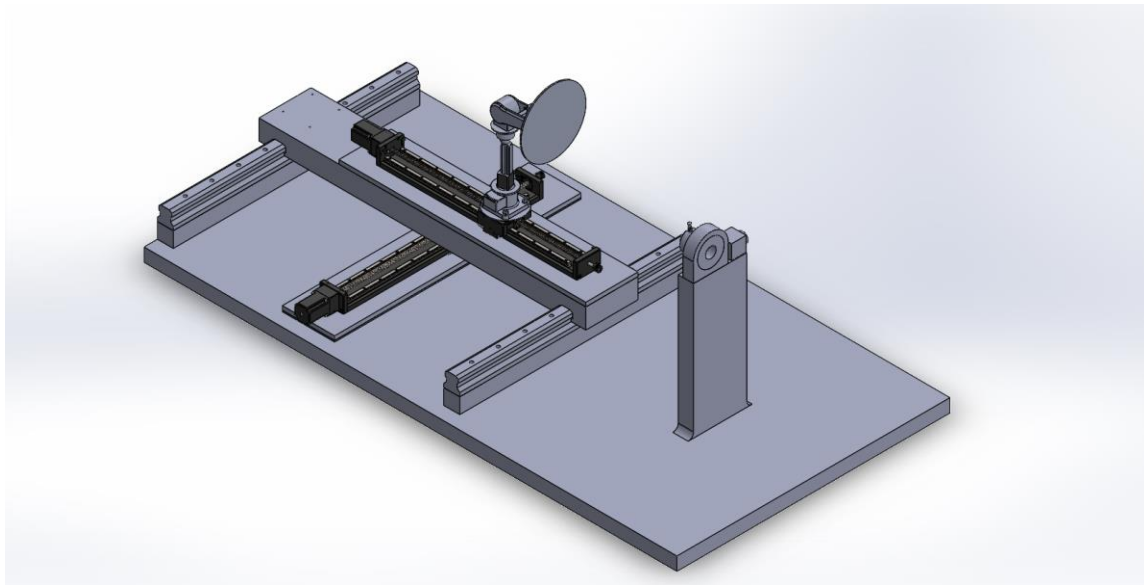


Figure 22: 3D CAD Model of 5DOF Grinding Wheel Arm Design (Isometric View)

4. Selection of Final Concept

4.1 Decision Matrix

The decision matrix utilized by the team weighs the criteria based on its importance and how effective it addresses the problem statement. The most important criterion is weighed 5 and the least important is weighed 1. Each solution is then ranked accordingly based on how it satisfies the criteria, whereby a higher rank represents better satisfaction of the criterion. Safety, efficiency, functionality, space, and cost are the five criteria chosen by the team which they found most relevant.

The safety criterion refers to how well the design protects the technician from carbide particles and possible physical injuries. The efficiency criterion refers to how relevant and efficient the design is from Halliburton's point of view. The functionality criterion refers to how realistic and practical the design will be. The space criterion refers to the amount of room required for the entire set up. Lastly, the cost criterion refers to the estimated price for each design in comparison to desktop Computer Numerical Control (CNC) machines with similar DOF.

Table 3: Decision Matrix

Criteria	Criteria Weightage	Enclosed 3DOF	Open System	Multi-Slot	5DOF
Safety	5	2	1	2	2
Efficiency	3	1	1	1*	1
Functionality	4	2	2	1	3
Space	2	2	1	3	3
Cost	1	1	2	3	4
Total Score		23	20	26	35

Note: There is an asterisk on the efficiency score for the Multi-Slot Gundrill Support design because it is deemed to be inefficient for Halliburton's situation. However, for organizations that specialize in regrinding of gundrills, this design can be regarded as a relatively more efficient solution for their process.

From Table 3, it is evident that the 5DOF grinding wheel design attained a total score of 35, which is the highest score among all the designs. Hence, moving forward, the team decided to proceed with the 5DOF grinding wheel design.

4.2 Modifications and Final Design

The final design is an improved version of the 5DOF grinding wheel design which stood out from the decision matrix utilized from the previous section. Figure 23 shows the 3D sketch of the finalised design.

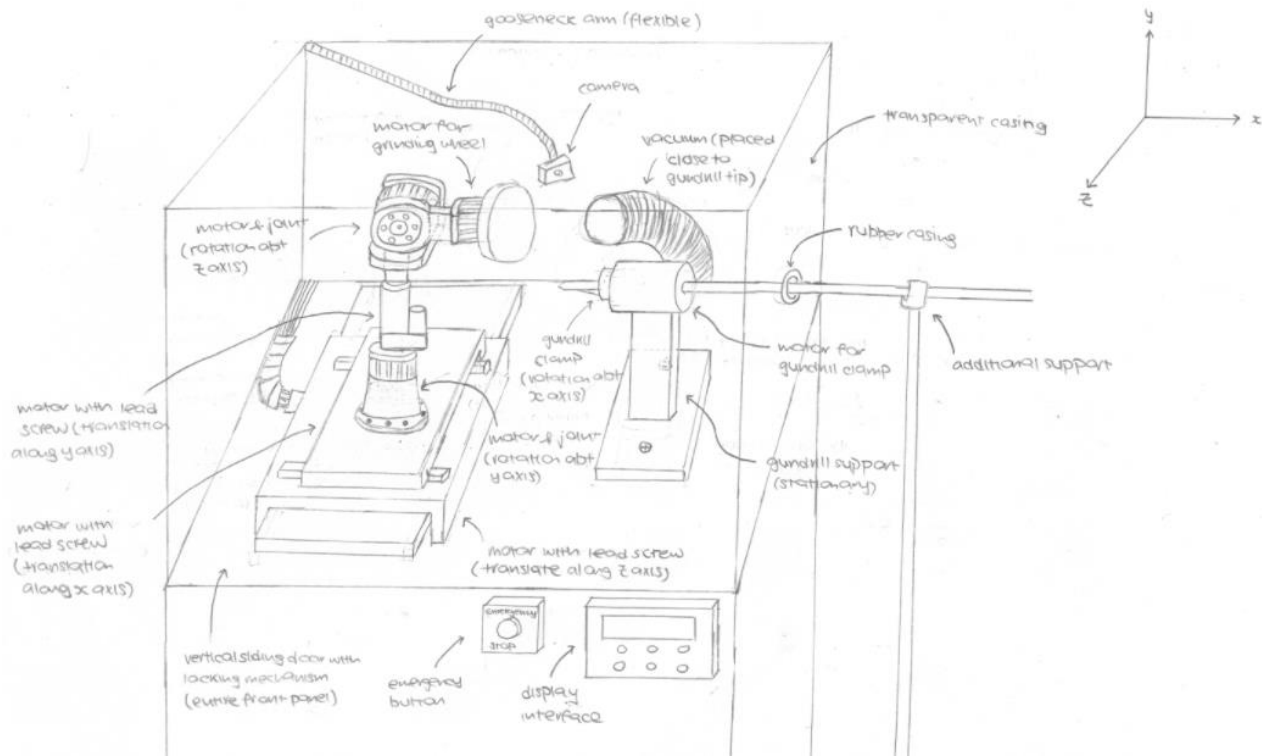


Figure 23: Sketch of Final Design

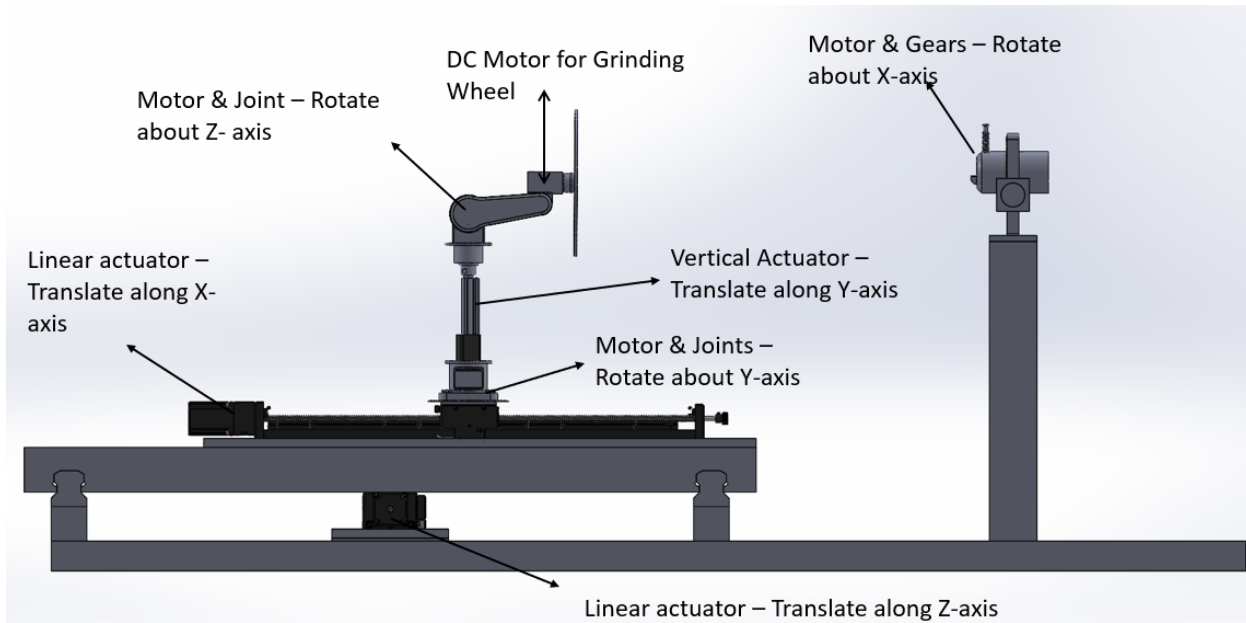


Figure 24: 3D CAD Model of Final Design (Front View)

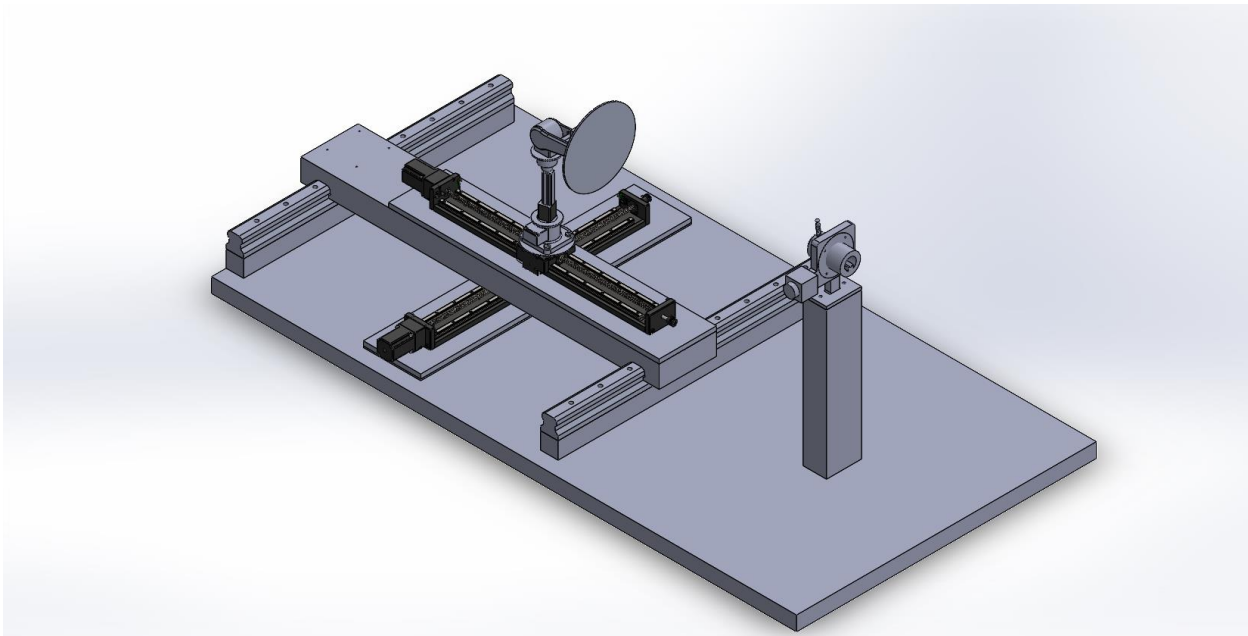


Figure 25: 3D CAD model of Final Design (Isometric View)

Modification was done on the design based on the suggestions and feedback given by the team's mentoring professor, the technicians and management at Halliburton as well as several staffs from SimTech and NUS.

The modifications of the design include:

1. Inclusion of emergency stop features which is an essential requirement on such setups.
2. Change of grinding wheel to a replaceable grinding wheel, which is preferably easily bought off the shelf.
3. Inclusion of vertical sliding door to allow technicians to tighten clamp and increase the ease of maintenance and replacement of grinding wheel. Vertical sliding door also requires less space compared to a conventional door that opens outwards.
4. Movement of industrial grade vacuum such that it is closer to the gundrill support for better suction of carbide particles.
5. A gundrill support with a smaller width and tapered design to consider shorter gundrills and to prevent obstruction to the grinding wheel during the grinding process.
6. Inclusion of camera with gooseneck arm to aid in visual inspections.

4.3 Revised Final Design

After discussion with various suppliers and running simulations (refer to section 7 below), the team came to realise the problems with having individual motors and actuators for each degree of freedom. The joints between the motors must be customised and manufactured, resulting in significant drawbacks such as the lack of rigidity and strength at the fabricated joints of the grinding wheel mount, which compromises the structural integrity. By manufacturing a completely new component, the amount of payload and forces that the fabricated parts can withstand are unknown. This could pose a problem due to the grinding force and vibration caused by the high rotational speed of the grinding wheel, which could lead to failure of the joints.

In addition, the use of individual motors increases the payload of the grinder setup which poses additional load requirements to the base motors. The team was also advised to implement a belt pulley system for the rotation about the y-axis and this requires a larger mounting area, rendering the design impractical due to space constraints. Moreover, the excessive usage of bolts and fasteners could lead to stress concentration on the joints, further compromising the structural integrity of the setup.

To resolve these issues, the team resorted to using a more expensive option: industrial robotic arm. Although the cost of robotic arms can be considerably higher, it has higher rigidity and strength as they are manufactured for purposes such as drilling, polishing, and grinding. In fact, as these manufacturers specialize in fabricating industrial robotic arms, many rounds of simulation and physical product testing have been conducted, which would eliminate the risk of failures that could be present in the design should the team decide to fabricate from scratch. Therefore, by using robotic arms, structural integrity is guaranteed, the risk of failure is eliminated, and safety is assured.

To attach the motor and the grinding wheel onto the industrial robotic arm, a customized motor bracket is required.

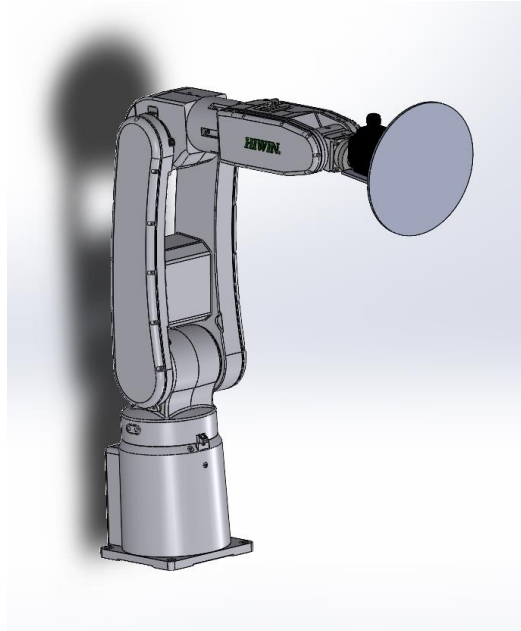


Figure 26: 3D CAD model of Industrial Robotic Arm

The team also faced another challenge in the fabrication of the original gundrill support design. The motor attached to the side of the gundrill support creates unnecessary moment. Furthermore, due to its orientation, there would be difficulties in transferring the rotational motion of the motor to the gundrill clamp. Options that were given were the use of bevel gears, worm gears or belt pulleys. However, the team felt that these gear and pulley systems would unnecessarily take up space and contribute extra load. In addition, if gear and pulley systems are used, more costs will be involved in fabricating a customized housing for these systems to protect them from exposure to carbide particles and coolant, during the grinding process. As a result, the team came to the decision of using a torque motor to allow for rotational motion in the gundrill support. Similarly, to attach the gundrill clamp to the torque motor, a customised motor bracket will be installed.

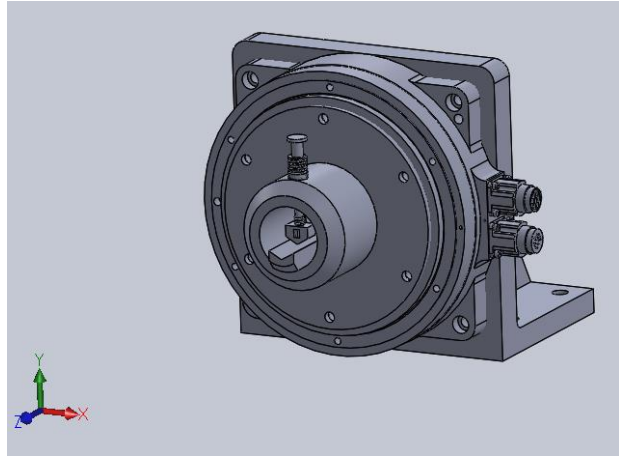


Figure 27: 3D CAD model of Torque Motor

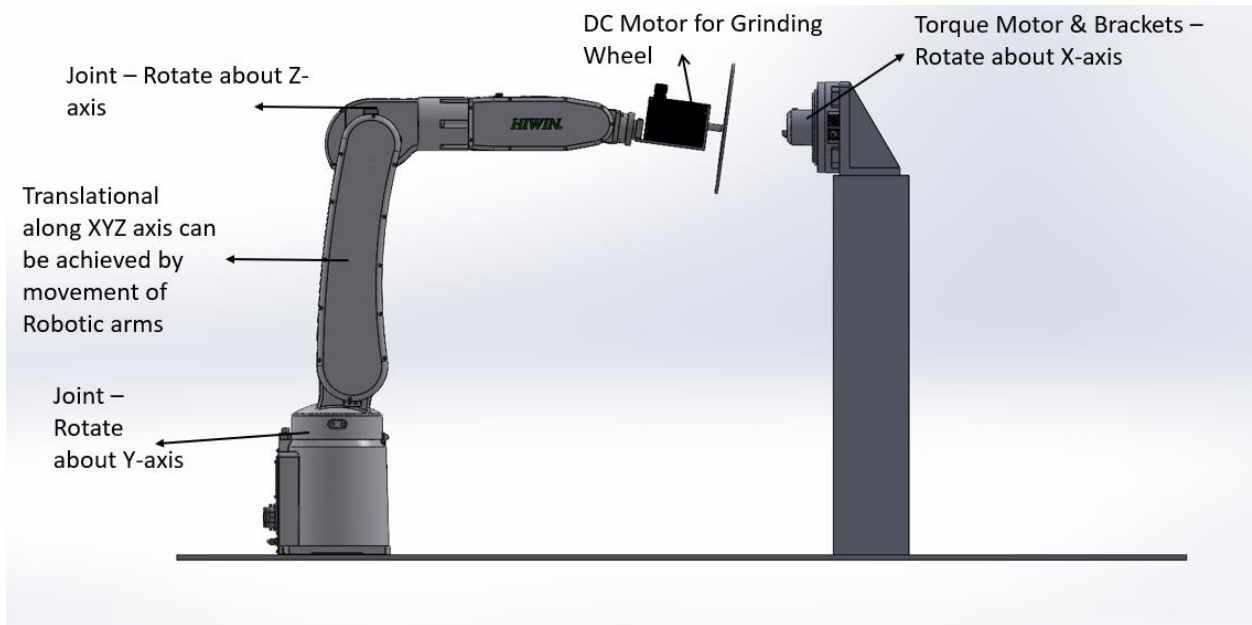


Figure 28: 3D CAD Model of Finalised Design (Front View)

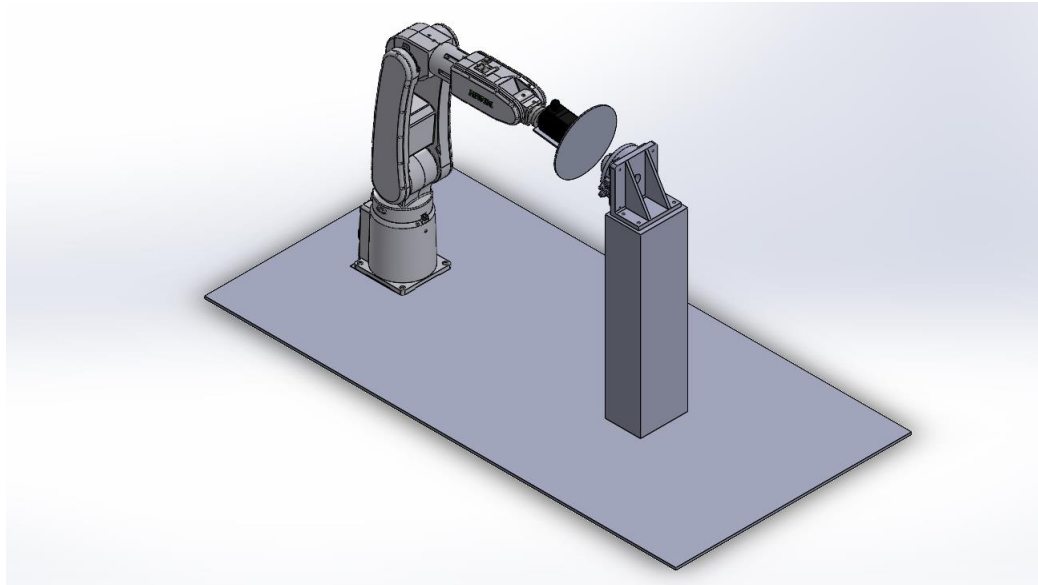


Figure 29: 3D CAD Model of Finalised Design (Isometric View)

4.4 Summary of final idea & pain points of current manual regrinding system

Table 44 summarises the pain points of the current manual regrinding system and features of the team's ideas that target the pain points as well as the corresponding project objective.

Table 4: Pain Points vs Features

Project Objective	Pain points	Features	
		Must-Have	Good-To-Have
Increase Accuracy	¼ diameter is not measured.	Camera	Microscope
	No precise method to check for angles on gundrill tip.	Gauge to measure the angles on gundrill tip.	Closed loop feedback system.
	Gun drills are prone to vibration.	Additional support	-
Reduce Health Hazard	Open system, exposing technicians to carbide particles.	Transparent casing with vacuum.	-
	Risk of injuries	Transparent casing and automation of system.	-
Increase Efficiency	Manpower is needed during the entire regrinding process.	Automation frees the technician up during the regrinding process.	-

4.4.1 Increase Accuracy

- 1.** $\frac{1}{4}$ diameter is not measured.

As shown earlier in the problem statement description, $\frac{1}{4}$ diameter is the most important measurement on the gundrill as it plays a significant role in the accuracy of the drilled hole taper. In the current SOP, the technicians are unable to measure with high accuracy as it is estimated using vernier callipers. Although the automation will aid in achieving higher precision, it is still necessary to install a camera for visual inspection for final checks before removing the gundrill from its support. It was also requested by Halliburton to have a means for visual inspection. On the other hand, a microscope will be a good-to-have feature which will come in handy when dealing with gundrills of an exceedingly small diameter.

- 2.** No precise method to check for angles.

The current regrinding method does not include a precise method to measure the final angle of the grinded gundrill. To ensure that the accuracy of the angles and finishing of the surface meets the required standard, precise gauges can be used to measure the angles while a good-to-have feature would be a closed loop feedback system, which will constantly feedback to the system to grind the gundrill until the required standards are met.

- 3.** Gundrills are prone to vibration.

In the current regrinding setup, there is no additional support to prevent the sagging and vibration of the gundrill due to the configuration of the conventional gundrill support. After implementing the new design, the gundrill support will not pitch and yaw, hence, an additional support can be installed near the tail of the gundrill. The support will reduce vibrations caused by grinding forces.

4.4.2 Reduce Health Hazard

- a)** Open system exposes technicians to carbide particles.

Even with the protection from N95 mask and the vacuum system, carbide particles can still land onto the technician's clothes and belongings, which can be harmful in the case whereby these harmful particles are consumed or inhaled by accident. The transparent casing together with a

vacuum is essential as it can minimise the contact between the technician and the carbide particles and reduce carbide particles in the environment by enclosing the work area.

b) Risk of injuries.

With the use of a transparent casing, it protects the technicians from the carbide particles as well as any breakage of equipment during the regrinding process. Automation also reduces the technician's contact with the grinding machine, minimising the risk of injuries. Hence, both features are essential in the prevention of injuries.

4.4.3 Increase Efficiency

a) Manpower is needed during the entire regrinding process.

In the current regrinding procedure, the technician must control the movement of both the grinding wheel and gundrill support manually. After securing the gundrill onto the clamp, the gundrill support will be adjusted to the desired angle and locked in position. The technician will then adjust the height of the grinding wheel accordingly and feed the wheel towards the gundrill tip to commence the grinding process. Automation of this manual process would improve efficiency. In the automated process, manpower will only be required to mount and dismount the gundrill from its clamp, which will free up the technicians for other tasks during the grinding process.

4.4.4 Other features

Additional features such as emergency stop features, sliding doors on casing with automated safety lock, replaceable grinding wheel, display interface and the relevant automation software are must-have features to ensure a safe and lasting operation. Although it is good to have an automated clamp, it is deemed as a secondary priority as the clamping action can be accomplished by technicians with ease.

5. Detailed calculations of Final Concept

5.1 Assumptions

- a) Diamond portion of the grinder does not add significant weight to the bearing load of the arm.
- b) A Safety Factor of 2 is used.
- c) Assume no chip is produced during the regrinding process.

5.2 Known Variables

- a) Range of diameters of commonly used gundrills at Halliburton is 3.58 - 12.7mm.
- b) Specific Grinding Energy of tungsten carbide is $4.15 \times 10^{10} \text{ J/m}^3$

5.3 Set Variables

These are the variables set by the team:

- a) Cutting speed of 25 m/s
- b) Diameter of grinding wheel is less than or equals to 10 cm.
- c) Feed Rate of 0.008333 m/s (500mm/min)
- d) Depth of Cut of 0.02mm
- e) Width of Cut of 13mm
- f) Rotational speed of 2860 RPM

5.4 Calculation of Power

Power, P, is calculated with the two formulas below. MRR refers to the material removal rate and is a product of the feed rate (f), depth of cut (d), and width of cut (b). Power required (P) is a product of the specific grinding energy of tungsten carbide (u) and the material removal rate (MRR).

$$MRR = f \times d \times b$$

$$P = u \times MRR$$

$$= u \times f \times d \times b$$

$$= 4.15 \times 10^{10} \times 0.008333 \times 0.00002 \times 0.013$$

$$= 89.913 W$$

Therefore, the calculated power requirement is 89.913W.

5.5 Calculation of Torque

Torque is calculated from the formula below, using the power and the angular velocity computed.

Torque is defined as the ratio of Power required (P) to the angular velocity of the grinding wheel (w).

$$T = \frac{P}{\omega}$$

$$= \frac{89.913}{2860 \times \frac{2\pi}{60}}$$

$$= 0.300 Nm$$

$$T_{SF} = 0.300 \times 2$$

$$= 0.600 Nm$$

5.6 Calculation of Grinding Force

The total grinding force is computed using the formula shown below. The total grinding force is defined as the ratio of the power required (P) to the cutting speed of the grinding wheel (v).

$$F_{grinding} = \frac{P}{v}$$

$$= \frac{89.913}{25}$$

$$= 3.597 N$$

$$F_{grinding(SF)} = 3.597 \times 2$$

$$= 7.194 N$$

6. Design of Components

This section illustrates the design iteration processes for components including the motor bracket, gundrill clamp and spindle. Refer to section 7 for the Finite Element Analysis (FEA) of final components.

6.1 Motor Bracket

6.1.1 Initial Design

The purpose of the motor bracket is to hold the motor that drives the grinding wheel, and act as a connection between the robotic arm end effector and the grinding wheel. The initial design of the motor bracket is a U-shaped bracket with the taller side connected to the end effector of the robotic arm, and the shorter side connected to the spindle motor. This design is made to accommodate the size of a smaller spindle motor (Dremel). However, the small Dremel motor is unable to achieve the required RPM of 2860. As a result, this design is obsolete as the choice of motor has been changed.

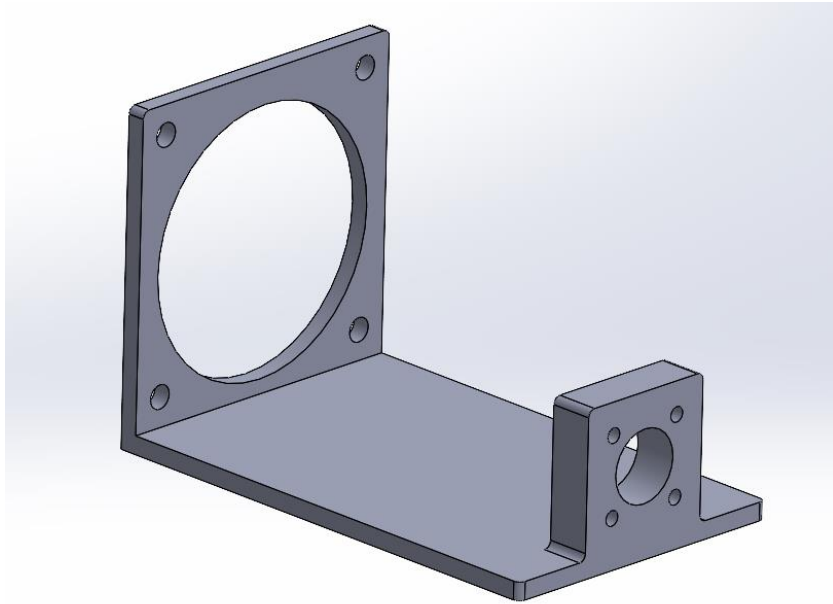


Figure 30: 3D CAD Model of Initial Bracket Design (Isometric View)

6.1.2 First Iteration

The first iteration of the motor bracket consists of both the 5mm and 8mm thick designs. For both designs, the material, height, width, and position of the holes are all identical, with the only difference being the thickness. This is to determine how the thickness of the motor bracket affects its strength. For this revision, the U-shaped idea is retained, and the sides of the bracket are adjusted to be of equal dimensions to simplify the design. Edge fillets are also added to reduce stress concentration and the distance between the two sides is reduced to better fit the motor. In addition, to facilitate motor assembly, a slot rather than a hole is created to allow the motor shaft to pass through easily.

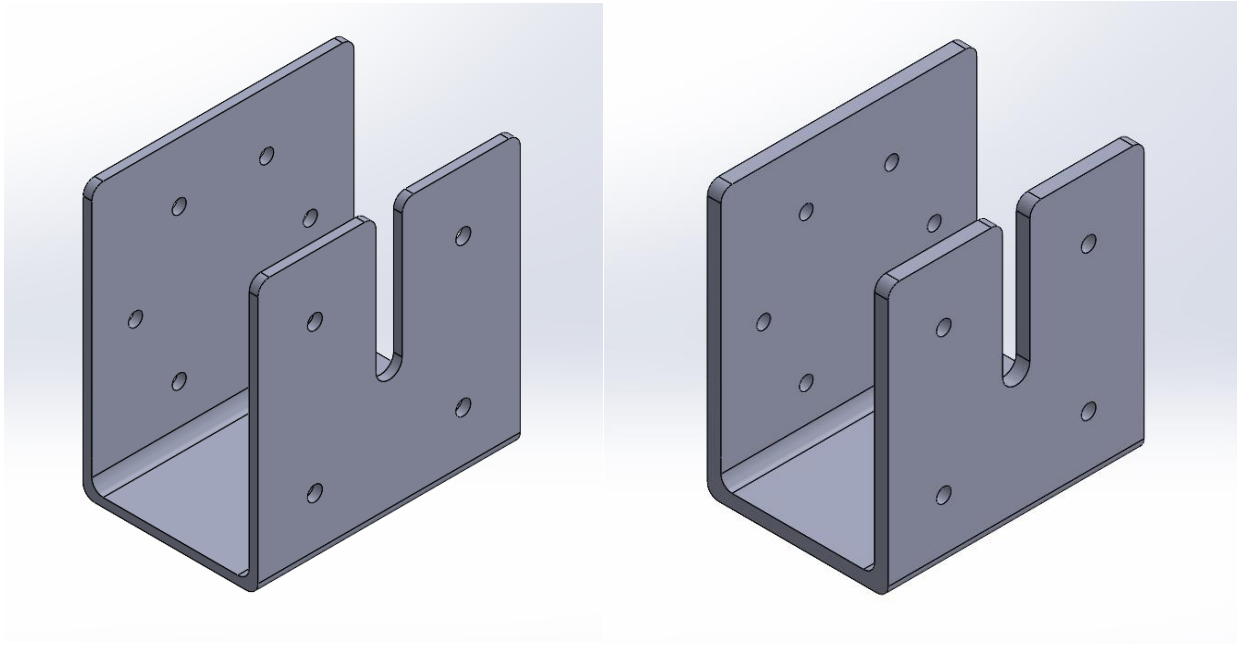


Figure 31: 3D CAD Model of 5mm (Top) and 8mm (Bottom) Bracket Design (Isometric View)

6.1.3 Second Iteration

Based on the simulation analysis performed on the 5mm and 8mm brackets as well as the challenges encountered during bracket fabrication, the team had to revise the designs. Both brackets can withstand the grinding loads calculated above, and hence the 5mm bracket design is selected as the final idea to save cost and material. However, for bending of the bracket to take place in order to fabricate it, the height of one side must be reduced as requested by the fabricator. To address this issue, the design is further improved by extending the length of the middle horizontal portion to 100mm, providing enough clearance for the bending tool. Mild steel was chosen as the material for the motor bracket, due to its strength and toughness, which was sufficient for the application.

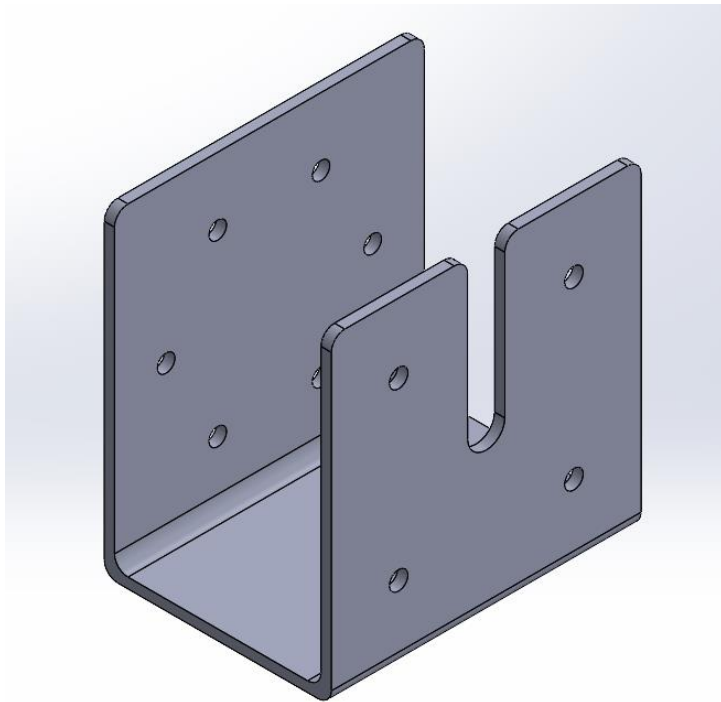


Figure 32: 3D CAD Model of Final Bracket Design (Isometric View)

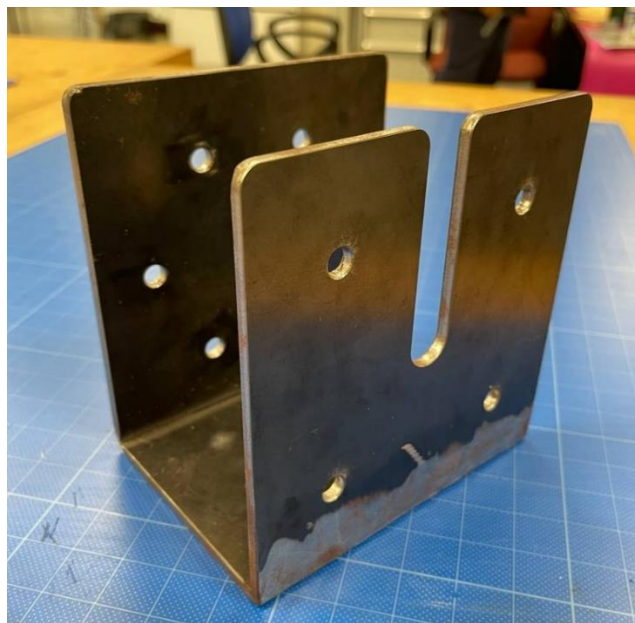


Figure 33: Final Bracket Design

6.2 Gundrill Clamp

6.2.1 Initial Design

The purpose of the gundrill clamp is to hold the gundrill during the regrinding procedure. The initial design of the gundrill clamp consists of a cylinder clamp, motor, housing for the bevel gears and a base support. However, there are some design flaws that might affect long-term usage. One of the major flaws of this design is that it can cause unnecessary moment due to the displacement of the motor. Furthermore, it is also difficult to replace the bevel gears as they are located beneath the housing. To eliminate the flaws in this design, the robotic arm supplier, Hiwin, introduced a new torque motor as shown in Figure 35. Hence, a new design was created to accommodate the new torque motor.

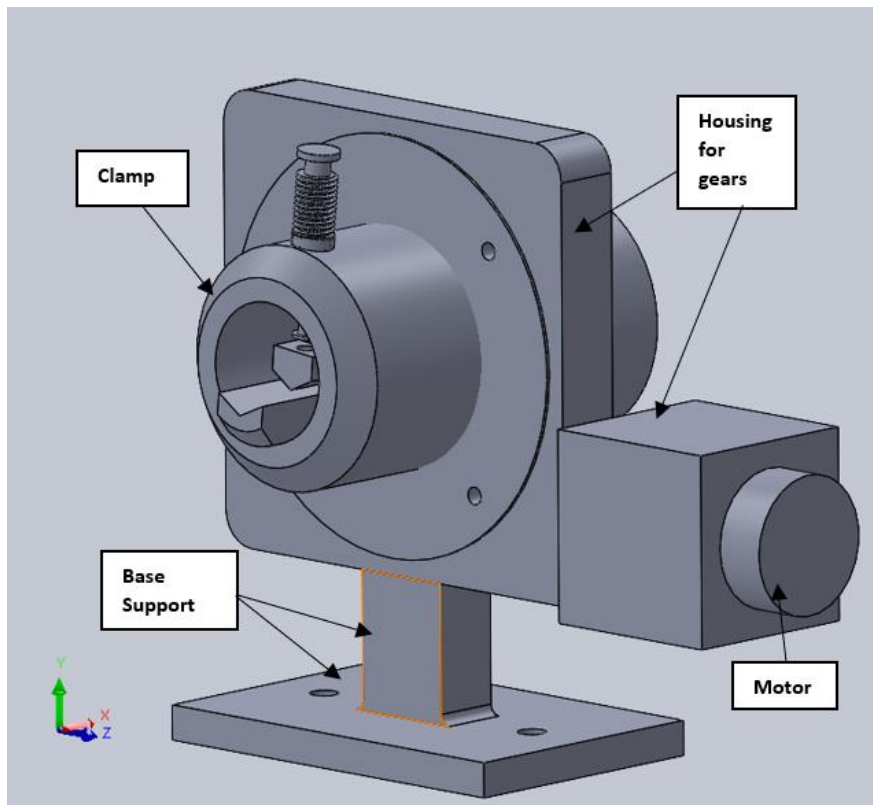


Figure 34: 3D CAD Model of Initial Gundrill Clamp Design (Isometric View)

6.2.2 First Iteration

Compared to the initial design, the first iteration design is more compact. It includes a cylindrical clamp with circular base, torque motor and a L-shaped bracket. The clamp is fastened onto the

torque motor with six M6 fasteners and the back of the torque motor is attached to the L-bracket with four M6 fasteners. Lastly, the bracket will be fastened down to the worktable. This design eliminates the unnecessary moment that was present in the initial design.

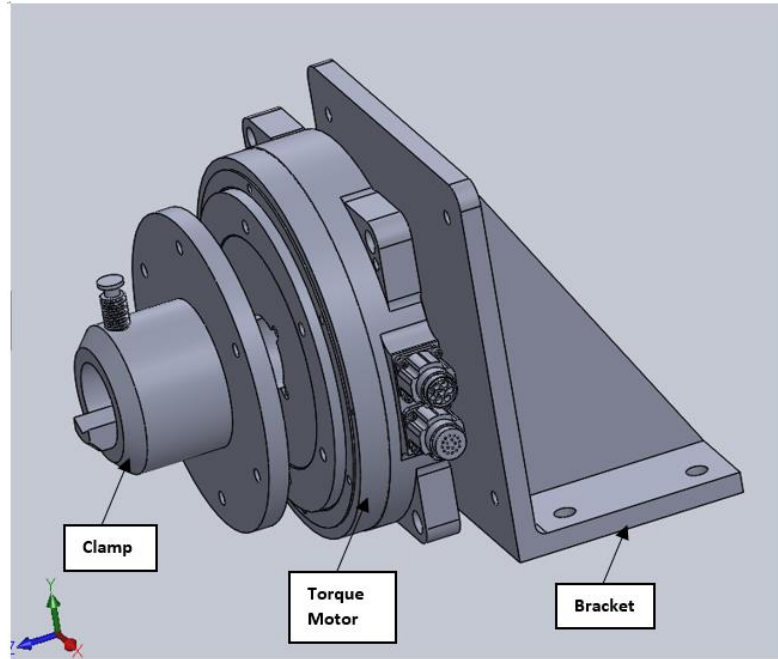


Figure 35: 3D CAD Model of Final Gundrill Clamp Design (Isometric View)

6.3 Spindle

6.3.1 Initial Design

The spindle serves as a support for the grinding wheel and the initial spindle design utilises the keyway principle to restrict relative movement between the motor shaft and the spindle. Once the spindle is mounted onto the motor shaft, a key is inserted into the keyway, locking and tightening the component securely. A 'D' shaped hole is also cut out according to the geometry of the motor shaft to further prevent relative rotation. A set screw is then added to offer additional locking of the spindle onto the motor shaft. However, this idea may be overdesigned for the application due to the extra locking mechanisms. Having a keyway permanently fixes the spindle onto the motor shaft, making removal afterwards extremely difficult. It also reduces shaft strength due to the stress points introduced. Inserting the key would require hammering which could potentially damage the motor. Furthermore, as the keyway is no longer widely used, it is hard to manufacture, hence a design revision is required.

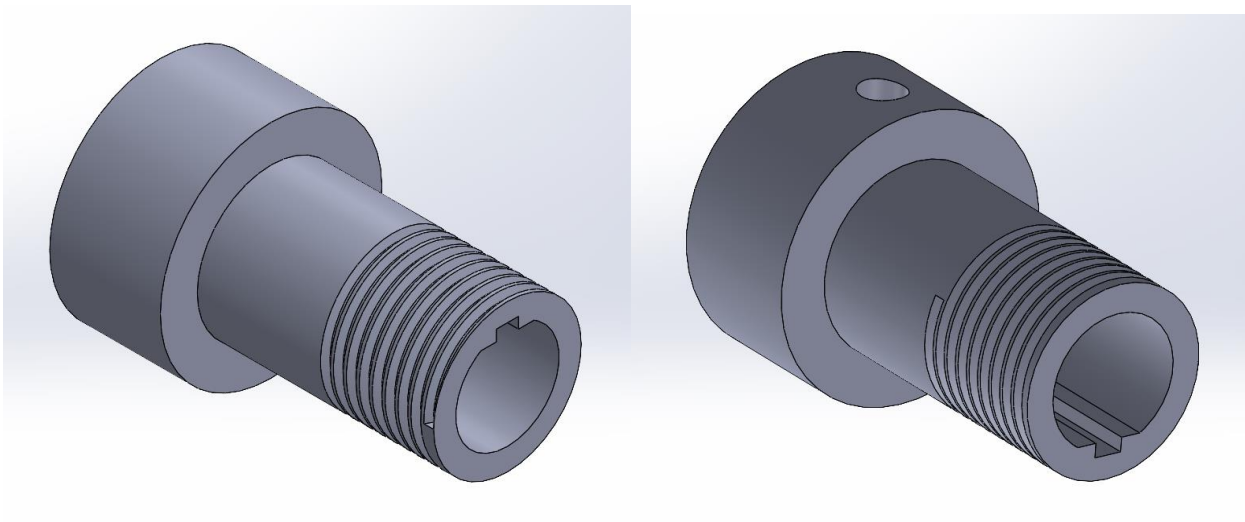


Figure 36: 3D CAD Model of Initial Spindle Design (Isometric View)

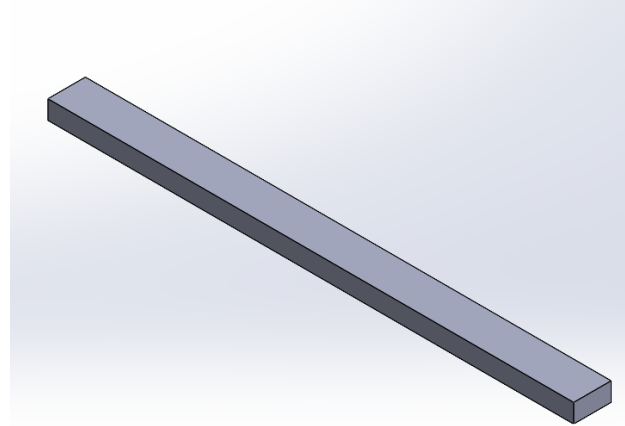


Figure 37: 3D CAD Model of Spindle Key (Isometric View)

6.3.2 First Iteration

To resolve the problems faced in the initial design, the keyway feature is removed. The original position of the M5 set screw is also shifted, and it is replaced by two smaller M3 set screws. This allows the set screws to rest on the flat portion of the motor shaft, improving contact and effectiveness. Having the 'D' shaped cut-out and the set screws are sufficient to secure the spindle to the motor shaft and prevent any rotational slip during the regrinding process. High carbon tool steel was chosen as the material for the spindle, due to its high wear resistance, which was desirable for the application.

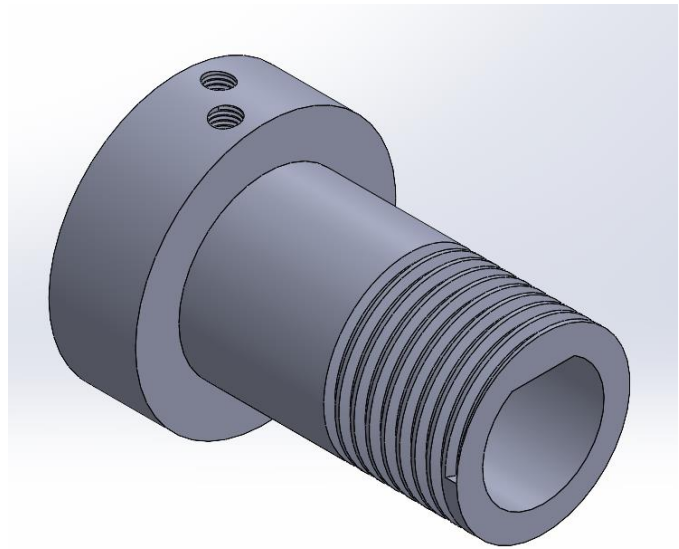


Figure 38: 3D CAD Model of Final Spindle Design (Isometric View)



Figure 39: Final Spindle Design

7. Simulation

7.1 Grinding Wheel Arm Simulation

A Finite Element Analysis (FEA) was conducted on the grinding wheel arm model. The objective of this FEA study is to determine the high-stress concentration regions within the grinding wheel arm and find out whether the model will fail under the applied loading conditions during the process of grinding.

Two sub-studies were conducted to obtain more definitive results for the FEA study. The first sub-study was conducted to analyse the top portion of the grinding wheel arm, which is close to the grinding wheel (surface where external load is applied to). The second sub-study was conducted on the entire grinding wheel arm assembly to pinpoint potential regions of failure.

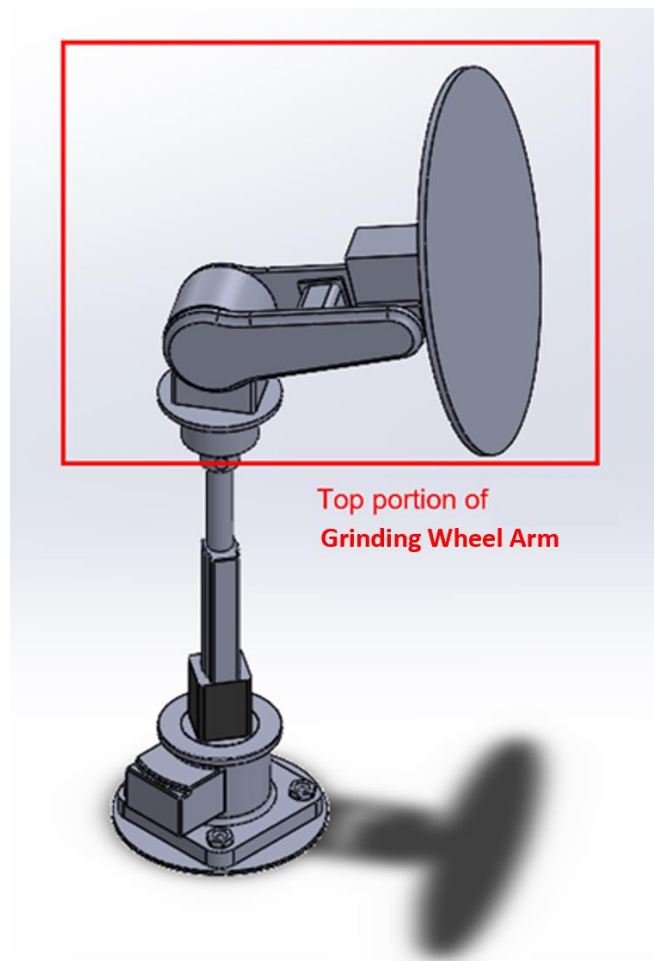


Figure 40: Grinding Wheel Arm Assembly Model for Simulation

Pertaining to building the FEA model for the grinding wheel arm, there are some important considerations to be considered, which could affect the results significantly.

Firstly, the grinding wheel will be in contact with the carbide tip of the gun drill during the process of grinding. Hence, there is an external load applied to the face of the grinding wheel, and it is assumed to be a distributed force.

Secondly, the materials of the components of the grinding wheel arm assembly are Alloy Steel, which has the following material properties: Young's Modulus (E) = 210GPa, Poisson's ratio (ν) = 0.28, density (ρ) = 7700kg/m³, and yield strength (σ_{yield}) = 0.6204GPa. For the grinding wheel itself, the material used is similar to diamond in terms of the following material properties: Young's Modulus (E) = 1050GPa, Poisson's ratio (ν) = 0.18 and density (ρ) = 3440kg/m³.

Thirdly, at maximum load, the stress level of the grinding wheel arm must be less than the maximum allowable stress, which is its yield strength factored by a safety factor (SF) of 2.0. The formula for safety factor (SF) is SF = Yield strength/Maximum allowable stress.

7.1.1 Sub-study 1: Static stress analysis of top portion of grinding wheel arm

For this analysis, only the components shown in the figure below are included in the analysis. The constraint imposed is that the bottom round shaft is fixed with a 'Fixed Geometry' fixture. An external uniform load of 8N (rounded up from calculated grinding force of 7.194N) is applied on the face of the grinding wheel, with the force direction normal to its surface. For the mesh density, blended curvature-based meshing was used. Mesh control with finer mesh density was applied to regions with high stress concentration, as depicted in the figure below.

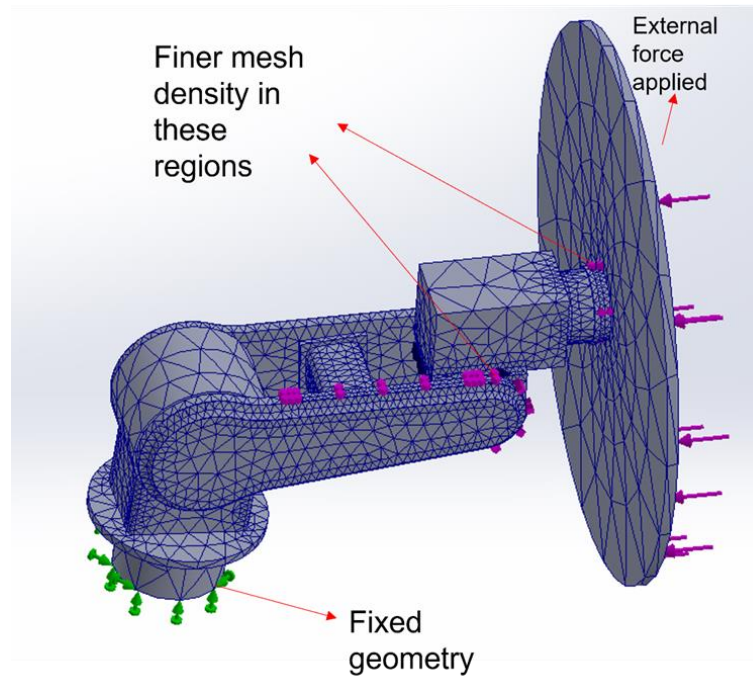


Figure 41: Mesh Density of Top Portion of Grinding Wheel Arm

For this sub-study, the maximum von Mises stress experienced is $3.594e+04$ N/m² at the connection between the grinding wheel and the shaft of the motor driving it. From the results illustrated in the figure below, it is also evident that there is a considerable amount of stress at the region where the grinding wheel arm link is connected to the motor (shown by the red circle).

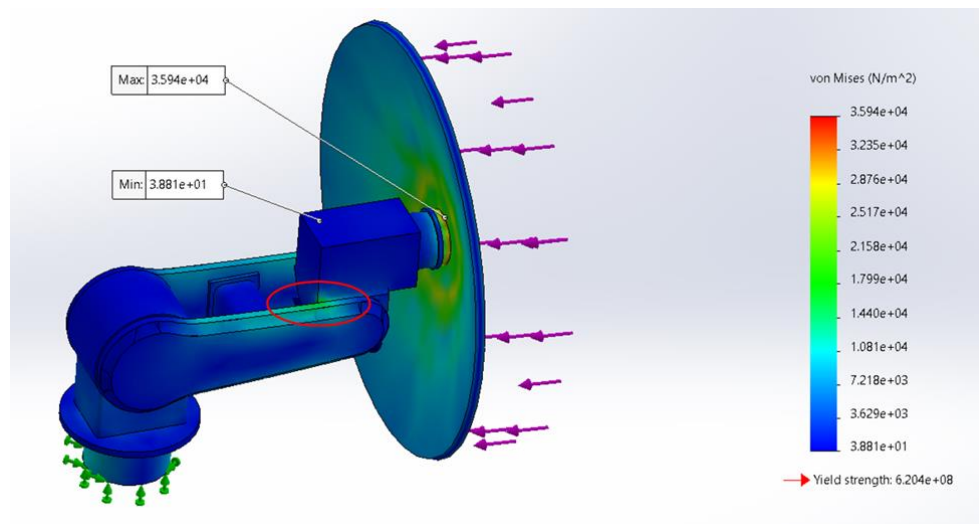


Figure 42: Von Mises Stress Results for Top Portion of Grinding Wheel Arm

7.1.2 Sub-study 2: Static-stress analysis of whole grinding wheel arm assembly

For this analysis, all the components in the grinding wheel arm assembly are included in the analysis. The constraint imposed is that the base plate of the grinding wheel arm is fixed with a 'Fixed Geometry' fixture. The same external load of 8N is applied on the face of the grinding wheel. Mesh control with finer mesh density was applied to the vertical linear actuator region, as depicted in the figure below.

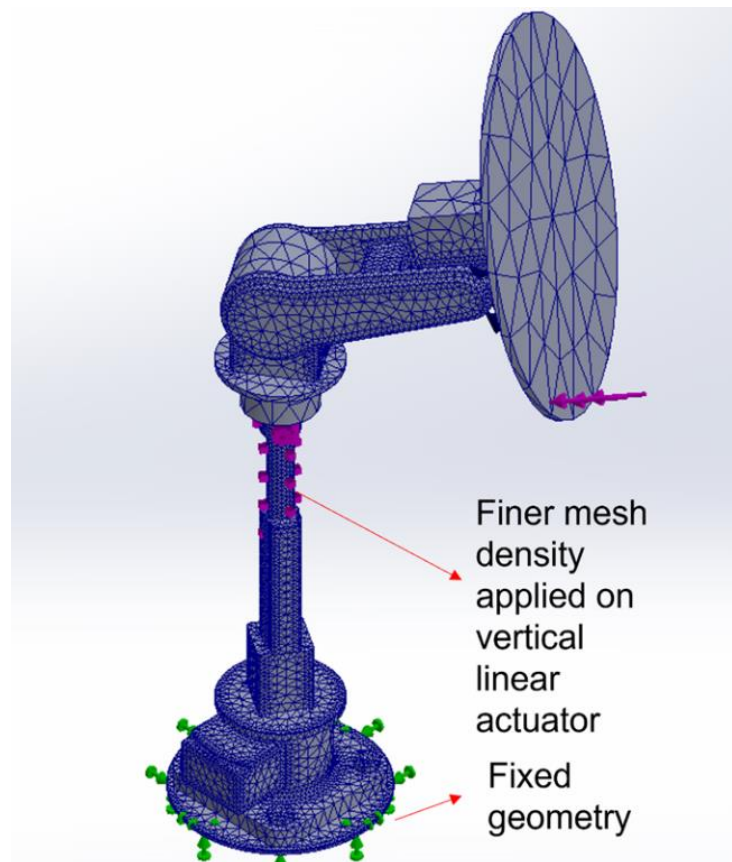


Figure 43: Mesh Density of Grinding Wheel Arm Assembly

For this sub-study, the maximum von Mises stress experienced is $9.542e+05$ N/m² at the rod of the vertical linear actuator. In fact, the stress concentration in that specific region is significantly higher than that in the other regions of the grinding wheel arm assembly.

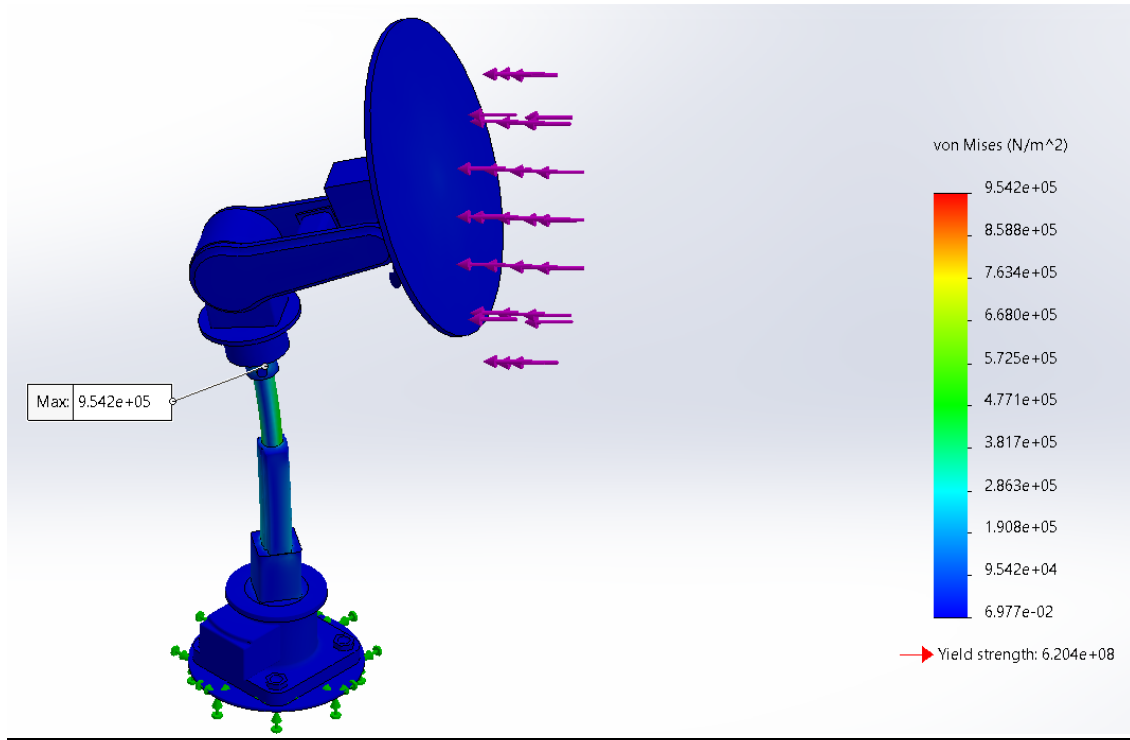


Figure 44: Von Mises Stress Results for Grinding Wheel Arm Assembly

In conclusion, the regions where the links of the grinding wheel arm are connected (joint areas where the grinding wheel arm is allowed to rotate) are generally areas which will experience higher stress compared to other regions. For the grinding wheel arm model, the region with the highest stress is the vertical linear actuator. The main reason is because the thickness of the linear actuator is small compared to the other components, and hence it is not as rigid as the other components. However, even with a safety factor of 2, the maximum von Mises stress at the linear actuator does not exceed the yield strength of the material used (alloy steel). Although the results of the simulation study may not be the most accurate due to many assumptions and much simplification, it is still critical to take note that more consideration should be put in place when designing the vertical linear actuator and the various joints of the grinding wheel arm assembly, as shown in the figure below.

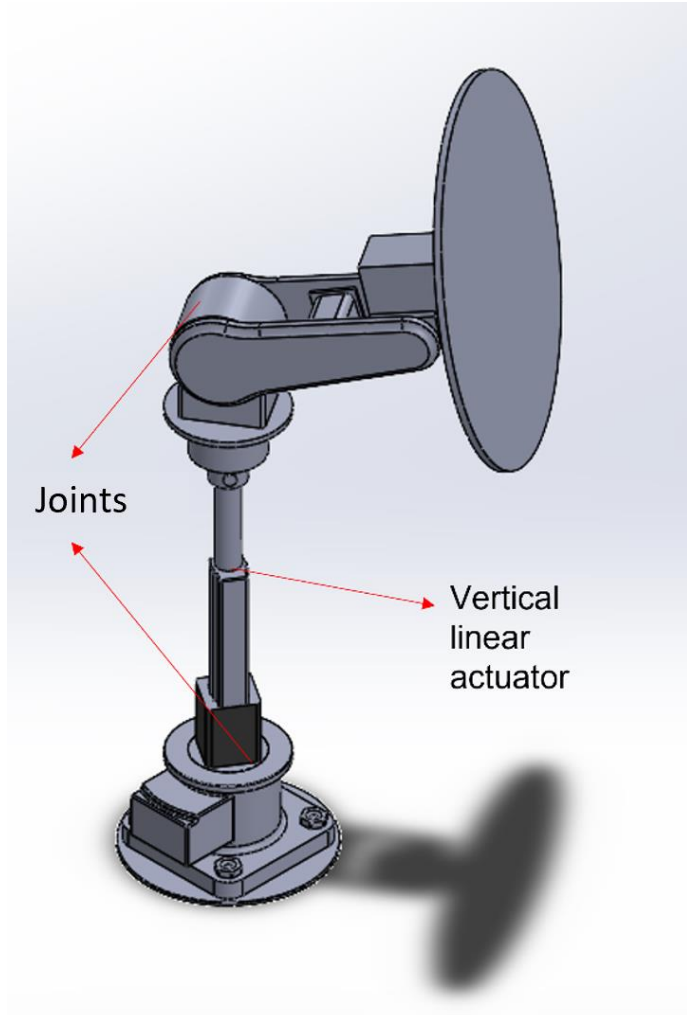


Figure 45: Joints for Grinding Wheel Arm Assembly

7.2 Bracket Simulation

7.2.1 Motor bracket

Analysis of the motor bracket was achieved by applying an external force of 50N onto the surface where the motor is attached. 50N does not represent the actual force on the motor bracket for the application, but it is an approximately large figure for which the team can conclude that the motor bracket is sufficiently strong, if the bracket does not fail during the simulation. The surface connected to the robotic arm's end effector is constrained with a 'Fixed Geometry' fixture. The material selected by the team for the motor bracket is mild steel. Mild steel was chosen due to its availability, strength, and toughness. After running the analysis, the results have shown that there is a higher stress concentration on the mid-section of the bracket, as shown in Figure 46.

Despite that, it is unlikely for the bracket to buckle as the maximum von mises stress experienced is 6.509e+06 N/m², which is lower than the yield strength of the mild steel material, 250e+06 N/m².

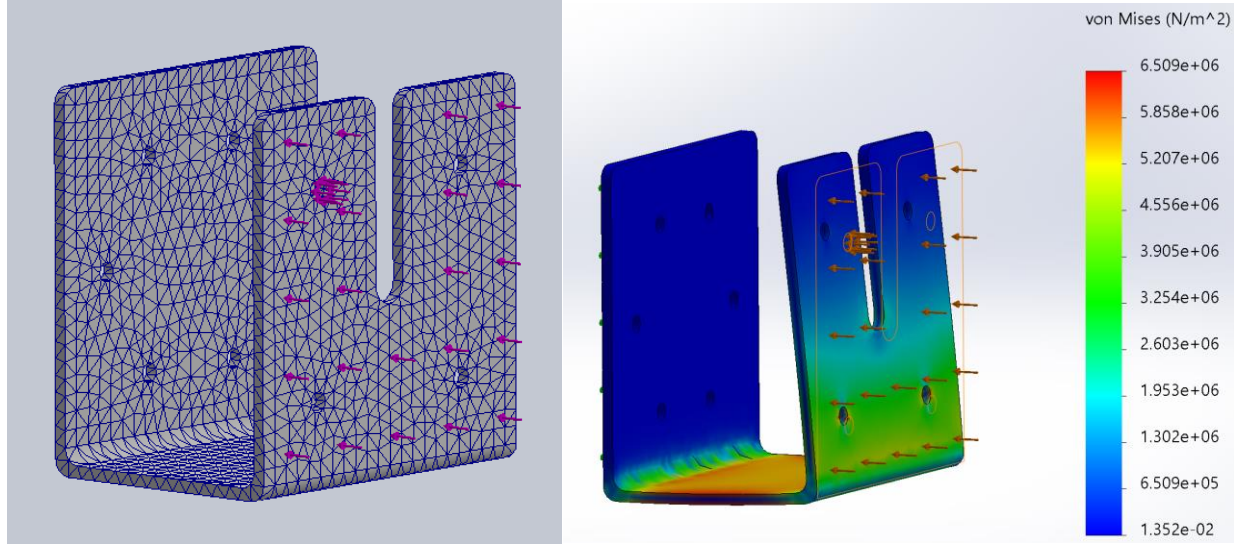


Figure 46: Simulation of Motor Bracket

7.2.2 L-bracket for Gundrill Support

For the analysis of the L-Bracket, a similar external force of 50N was applied onto the surface attached to the torque motor. Analysis was carried out on a fine mesh across the bracket. The bracket base was constrained with a ‘Fixed Geometry’ fixture. Likewise, mild steel was applied as the material of the bracket.

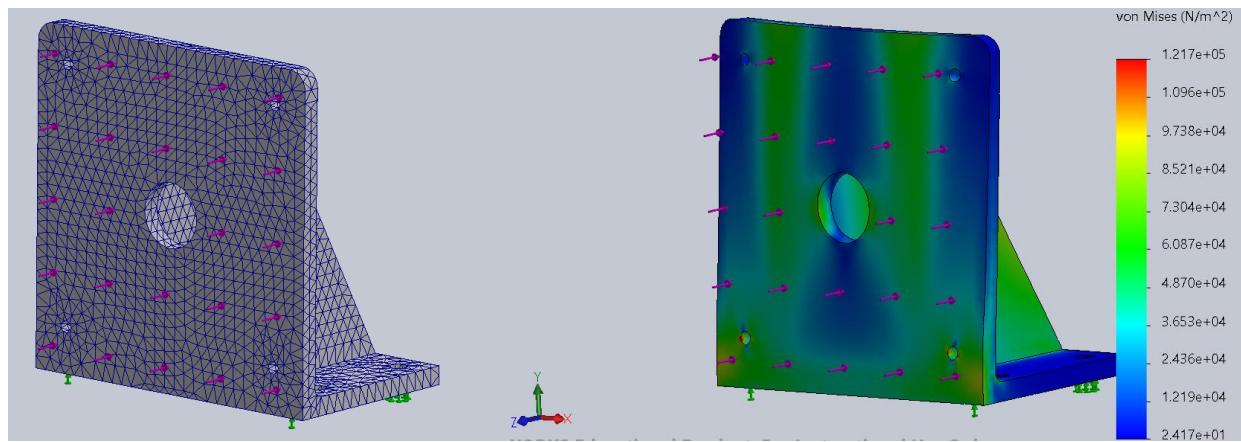


Figure 47: Simulation of L-Bracket

The FEA results illustrated that the maximum von mises stress experienced is $1.217\text{e+}06 \text{ N/m}^2$. This indicates that the bracket can withstand the 50N load safely as mild steel has a yield strength of $250\text{e+}06 \text{ N/m}^2$.

Since the torque motor will be attached onto this bracket, it is essential that the team also ensures that it can withstand a load of 50N safely. According to the torque motor specification sheet provided by the supplier, it can withstand a maximum axial load of 600N. Given that the supplier has conducted numerous rounds of rigorous testing of the actual product in addition to simulations, to accurately determine its current specifications, the data provided should be reliable and more accurate than the FEA results derived above.

8. Sourcing of Materials/Components

Components of the set up are selected based on constraints of the project and requirements set by Halliburton. Shown in Table 55 are the components that the team had sourced and attained quotations for at the time when the report was written.

Table 5: Bill of Material (Testing of Concept)

No.	Component name/ model	Description	Image	Supplier	Quantity	Quotation (SGD)	Total Cost (SGD)	Lead Time
1	BLV640NA-3 48V DC Motor	Motor to run grinding wheel.		Oriental Motor	1	\$802.50	\$802.50	6 Weeks
2	Motor Bracket	Used to mount the motor onto the robotic arm end effector.		Fujitson	1	\$101.65	\$95.00	1-2 Weeks

3	DC Power Supply + Cable Plug	Used to power the DC motor.		Kaichin Computer Systems Pte Ltd	1	\$433.35	\$433.35	Bought off the Shelf
4	Motor Spindle	Used as an adaptor to attach the grinding wheel onto the motor shaft.		Fabricated in NUS	1	-	-	-
5	TBT No 851248	15cm Diamond Grinding Wheel used to grind the gundrill tips.		Loaned from Halliburton	1	-	-	-

6	Gundrill Clamp	Used to clamp down workpiece during the testing procedure.		Loaned from SimTech	1	-	-	-
7	Kuka KR60 (Kuka Robotics)	Robotic Arm used for testing.		Loaned from SimTech	1	-	-	-
8	M14 Clamping Kit	Used to secure the gundrill support onto worktable.		Loaned from NUS Design Lab	1	-	-	-

9	Tachometer	Used to check grinding wheel rotational speed.		Loaned from NUS Advanced Manufacturing Lab	1	-	-	-
10	Vacuum (FA-430 Fume Extractor)	Used to remove carbide particles from the atmosphere.		Loaned from Design Lab	1	-	-	-
11	CC05IF-USB Communication Cable	Used to connect the motor driver to PC.		Loaned from Oriental Motor	1	-	-	-
Total: 1337.50								

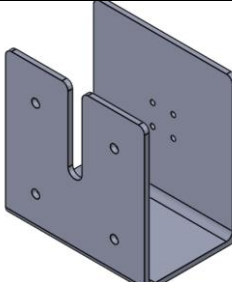
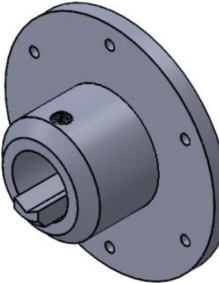
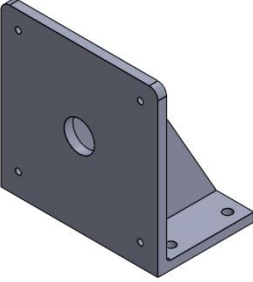
Table 6 shows the BOM for the actual implementation for the design. Motor, DC power supply and spindle are excluded from the BOM as it has already been purchased for the testing and can be re-used.

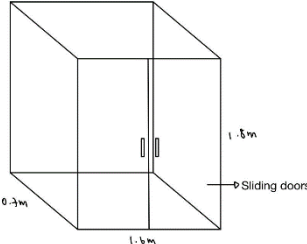
Table 6: Bill of Material (Actual Implementation)

No.	Component name/ model	Description	Image	Supplier	Quantity	Quotation (SGD)	Total Cost (SGD)	Lead Time
1	RA610-1355-GC	6-Axis Robotic Arm to mount grinding wheel onto (Software included).		Hiwin	1	40,000.00	40,000.00	2.5-3 Months
2	TMN-71	Torque Motor used for x-axis rotation on gun drill support (Driver included).		Hiwin	1	6,758.02	6,758.02	2.5-3 Months

3	GoPro Hero 5	Camera used for visual inspection.		Amazon	1	415.71	415.71	10-14 Days
4	Omron D40A (5m)	Compact non-contact door switch.		Monotaro	1	139.90	139.90	7 days
5	TBT No 851248 (Vallen)	15cm Diamond Grinding Wheel.		Pre-existing at Halliburton	1	-	-	-
6	Ball Bearing	Component for additional gundrill support to allow gundrill to rotate freely.		Amazon	1	5.00	5.00	7 Days

7	GoPro Super Suit for Hero5 Camera (AADIV-001)	Protective casing for camera for protection against carbide particles.		Amazon	1	55.61	55.61	10-14 Days
8	GoPro Gooseneck (ACMFN-001)	Gooseneck to allow for easy movement and adjustment for camera.		Amazon	1	40.00	40.00	10-14 Days
9	Vacuum	Used to remove carbide particles from the atmosphere.		Pre-existing at Halliburton	1	-	-	-

10	Motor Bracket	Used to mount the motor onto the robotic arm end effector.		Fujitson	1	\$101.65	\$101.65	2-3 Weeks
11	Gundrill Clamp	Used to hold the gundrill in place.		KS Precision	1	\$300.00	\$300.00	4-5 Weeks
12	L-Bracket	Used to secure torque motor.		KS Precision	1	\$260.00	\$260.00	4-5 Weeks

13	Robotic Enclosure	Used to prevent carbide particles from escaping.		Acrylicsm	1	\$1503.35	\$1503.35	7-14 Days
14	CC05IF-USB Communication Cable	Used to connect driver to PC.		Oriental Motor	1	\$133.75	\$133.75	7-10 Days
Total: 49,712.99								

9. Testing of Concept

As a proof of concept, the experiment was carried out on a robotic arm to perform actual grinding on a gundrill. A desktop robotic arm was not used as the team felt that it was insufficient to prove the design concept as actual grinding cannot be carried out. Furthermore, the addition of a desktop robotic arm would not be beneficial to the company, hence an industrial robotic arm was chosen instead.

The robotic arm used in the experiment is the KUKA KR60 located at the Advanced Robotic Centre (ARC) Laboratory which was loaned from SimTech. The robotic arm was programmed to perform the translational movement in all three axes and the rotational movement in the y and z-axes, identical to the finalised design idea. For experimental purposes, the torque motor was excluded as it would not significantly affect the results of the experiment and the x-axis rotation was carried out manually on the gundrill clamp.

The testing criteria used for the experiment were the time taken for the regrinding process and the accuracy of the regrind, which were two of the main points discussed in the problem statement. Testing criteria will be further elaborated in the following sections.

9.1 Electrical Connections

During the experiment, the motor was used to turn the grinding wheel at a rotational speed of 2860 RPM. The motor, BLV640NA, comes with a driver that was used to control the system. To start the motor running, the basic connections were the DC power supply (CN1), I/O signal connector (CN4), motor signal and power connectors (CN2, CN3) as they were needed to close the circuit.

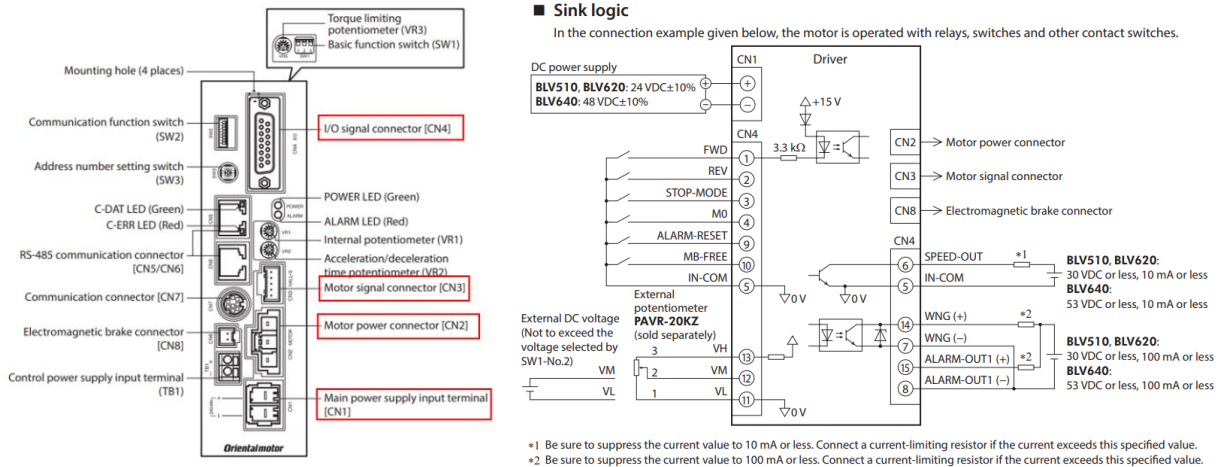


Figure 48: Driver Configuration

For the motor driver, the I/O signal connector required a 15-pin d-sub plug (male) and a switch to be soldered to the first and fifth pins to allow the clockwise rotation to take place. This configuration is shown below in Figure 49.

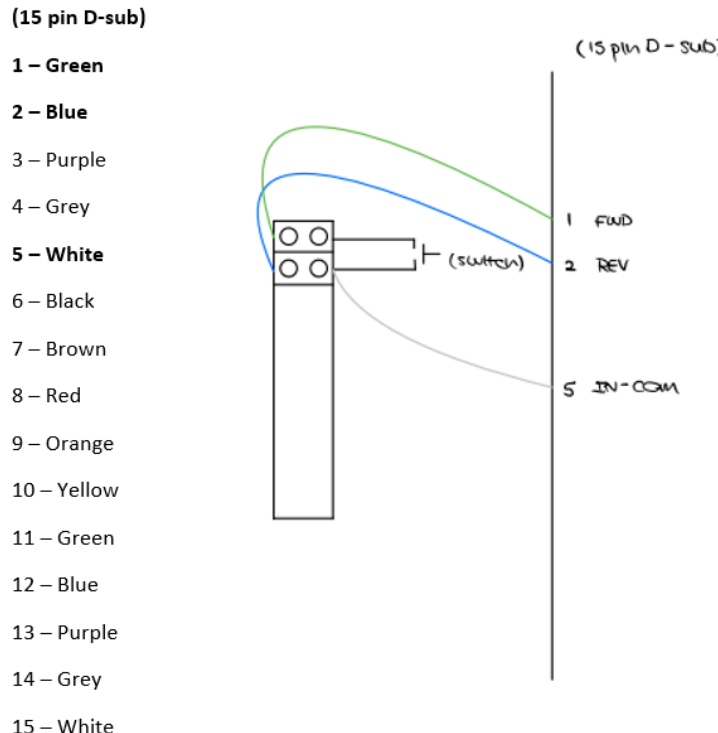


Figure 49: 15-Pin Configuration

An official communication cable, CC05IF-USB, was needed for the speed control software, MEXE02 and the communication cable was connected to CN7 port on the driver. Furthermore, the second and fifth pin of the I/O cable were connected to the circuit. The final electrical connections of the driver for the application are shown in Figure 5050.



Figure 50: Driver Electrical Connections

9.1.1 Speed control software interface: MEXE02

In the MEXE02 software, the speed was set to 2860 RPM. After the desired rotational speed was set, the data was written from PC to driver. Once the data was successfully transferred over to the driver, the motor would then automatically run at the input rotational speed when the switch was turned on.

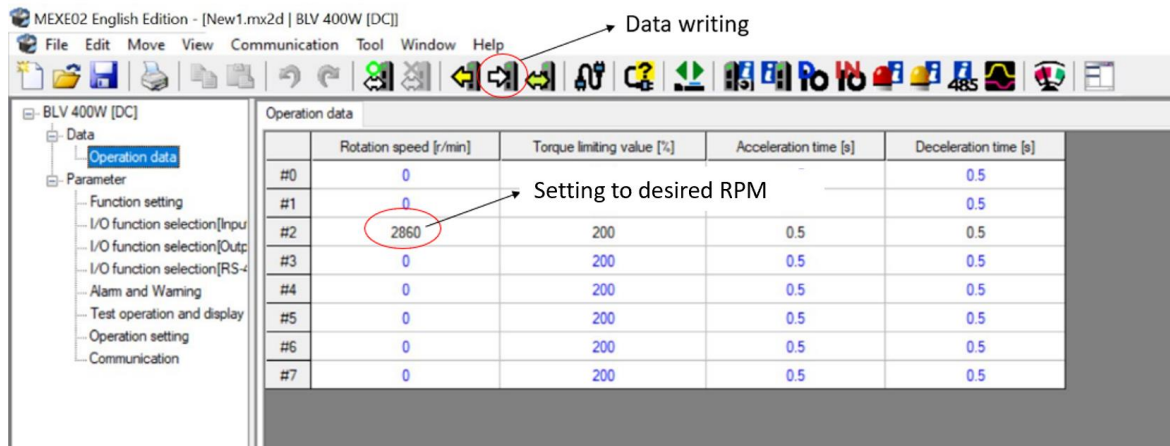


Figure 51: PC Display of Motor Software

When the motor was running, the software was able to monitor the motor speed at a given time, which was extremely useful in ensuring that the motor shaft was turning at the constant desired RPM, as shown in the real-time motor status illustrated in Figure 52 below.

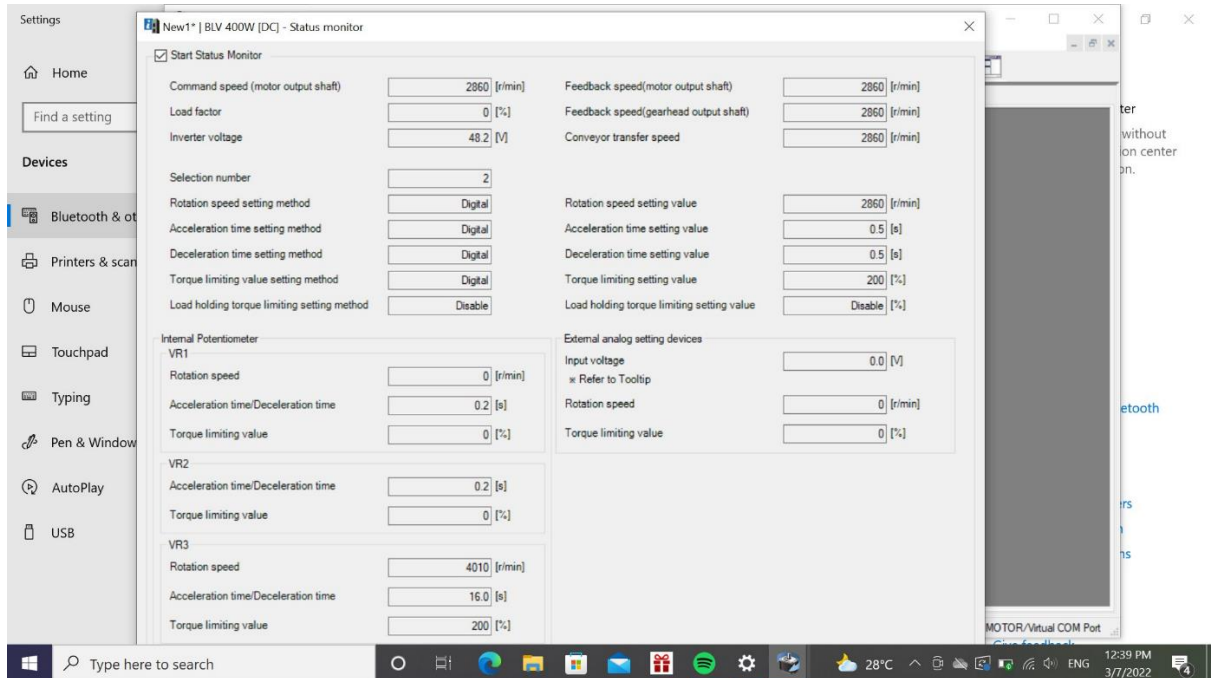


Figure 52: PC Display (Real-Time Motor Status)

9.2 Components for Testing

In this section, the individual components that make up the assembly for the testing of concept will be explained in detail. There are a total of 6 main individual components used for the testing at the NUS ARC Laboratory, namely the Kuka KR60 Robotic Arm, SDR-960-48 Power Supply, BLV640NA DC Motor and Driver, FA-430 Fume Extractor, Gundrill Clamp, Spindle, and Motor Bracket.

9.2.1 KUKA KR60 Robotic Arm

The main component in the assembly that carried out the automated regrinding of the gundrill is the KR60. The essential specifications of this robotic arm are its rated payload and repeatability, which is defined as the similarity of agreement between various positions reached by the end-effector for the same controlled position, repeated several times under the same conditions [16]. The rated payload for the KR60 is 60kg, which is greater than the required payload of approximately 6kg. In addition, its repeatability is ± 0.06 mm.

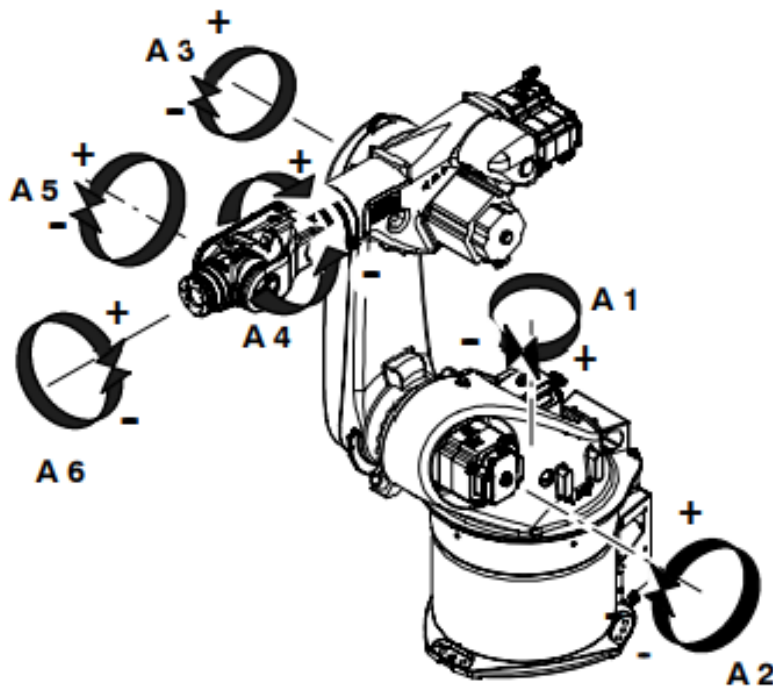


Figure 53: Robotic Arm Axis

Table 7: Robotic Arm Axis Motion and Speed

Axis	Range of Motion	Speed
1	$\pm 185^\circ$	$128^\circ/\text{s}$
2	$+35^\circ$ to -135°	$102^\circ/\text{s}$
3	$+158^\circ$ to -120°	$128^\circ/\text{s}$
4	$\pm 350^\circ$	$260^\circ/\text{s}$
5	$\pm 119^\circ$	$245^\circ/\text{s}$
6	$\pm 350^\circ$	$322^\circ/\text{s}$

The KR60 has six degrees of freedom, as indicated in the figure above. All the 6 axes are essential in controlling the angles essential for the regrinding procedure. From the chart above, axis 1 has a range of motion of $\pm 185^\circ$ and can move up to maximum speed of $128^\circ/\text{s}$. Axis 2 has a range of motion of $+35^\circ$ to -135° and can move up to a maximum speed of $102^\circ/\text{s}$. Axis 3 has a range of motion of $+158^\circ$ to -120° and can move up to a maximum speed of $128^\circ/\text{s}$. Axis 4 has a range of

motion of $\pm 350^\circ$ and can move up to a maximum speed of $260^\circ/\text{s}$. Axis 5 has a range of motion of $\pm 119^\circ$ and can move up to a maximum speed of $245^\circ/\text{s}$. Axis 6 has a range of motion of $\pm 350^\circ$, and can move up to a maximum speed of $322^\circ/\text{s}$. Given that the required range of motion for the testing application was much smaller than the robotic arm's range of motion, the KR60 was suitable for meeting the testing requirements.

9.2.2 SDR-960-48 Power Supply



Figure 54: Power Supply

Table 8: Power Supply Specification

Specifications	
DC Voltage	48V
Rated Current	20A
Current Range	0 - 20A
Rated Power	960W
Efficiency	94%
Safety Standards	UL508, TUV EN60950-1 approved

To power up the 48V DC motor used for driving the grinding wheel, the SDR-960-48 power supply was used. Matching the voltage of the motor, the power supply also has a DC voltage of 48V, a current range of 0 to 20A, and rated power of 960W. Although this power supply is considered

relatively heavy duty, it has certified safety standards. It is TUV EN60950-1 approved, and this standard is recognised and applies to mains- or battery-powered IT equipment, including electrical office machines, and associated equipment with rated voltages of up to 600 V.

9.2.3 BLV640NA DC Motor



Figure 55: Motor and Driver

Table 9: Motor Specifications

Specifications	
Rated Output Power	400W
Rated Voltage	48VDC
Rated Input Current	11A
Maximum Input Current	18A
Rated Torque	1.3N-m
Speed Control Range	100 – 4000 RPM

As mentioned earlier, after doing calculations, it was found that the desired RPM for the regrinding process was approximately 2860 RPM, in order to emulate the parameters of the current regrinding process carried out at Halliburton. From the chart, it is evident that the speed control range of the motor ranges from a minimum of 100 RPM to a maximum of 4000 RPM.

Therefore, the BLV640NA DC motor can run at the desired rotational speed and fulfils the testing requirements.

9.2.4 FA-430 Fume Extractor



Figure 56: Fume Extractor

To remove the carbide particles released due to grinding, the FA-430 Fume Extraction system was used as a makeshift vacuum system. The suction tube is placed on the gundrill clamp below the area where the grinding wheel contacts the gundrill during the regrinding process, as seen in Figure 56 above.

Table 10: Fume Extractor Specifications

Settings		
	Noise Level	Air Volume
HIGH	53dB	4.7m ³ /min
MEDIUM	50dB	3.7m ³ /min
LOW	44dB	2.8m ³ /min

Equipped with a High Efficiency Particulate Air (HEPA) filter, the FA-430 Fume Extractor is effective in filtering out 99.97% of particles greater than 0.3µm. For testing purposes, this fume extractor meets the requirements, given that the typical size of carbide particles is approximately

$0.8\mu\text{m}$ for micro-grains, and $1\mu\text{m}$ for fine grains. For comparison, the FA-430 Fume Extractor is strong enough to filter out solder smoke and solid dust. In addition, there are different suction settings for the fume extraction system. To ensure maximum effectiveness and reduce the risk of carbide particles being released into the air, the system was kept on at a HIGH setting, throughout the duration of the testing.

9.3 Physical Assembly

Figure 57 below shows the motor assembly. The motor assembly includes the motor, motor bracket, spindle and grinding wheel. The motor bracket was fastened to the KR60's end effector with the use of six M8 fastening screws while the motor was fastened onto the bracket with four M8 bolts and nuts. The spindle was fitted and tightened onto the motor shaft with its set screws. The spindle served as an adaptor to allow the grinding wheel to fit in tightly and to fasten the grinding wheel with a M12 nut.

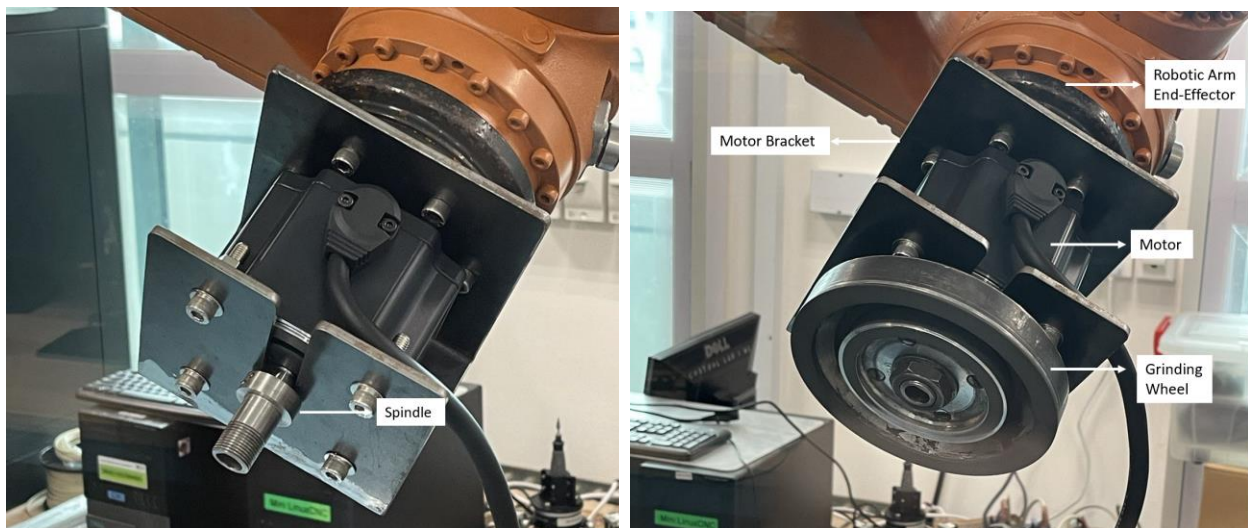


Figure 57: Motor Assembly

On the worktable side, a gundrill clamp was secured with an M14 T-slot Clamp. A vacuum (FA-430 Fume Extractor) was installed near the tip of the gundrill where the grinding took place. During grinding, the carbide tip gundrill (workpiece) was clamped down on the insert of the gundrill clamp, to ensure that it remained in position for grinding.

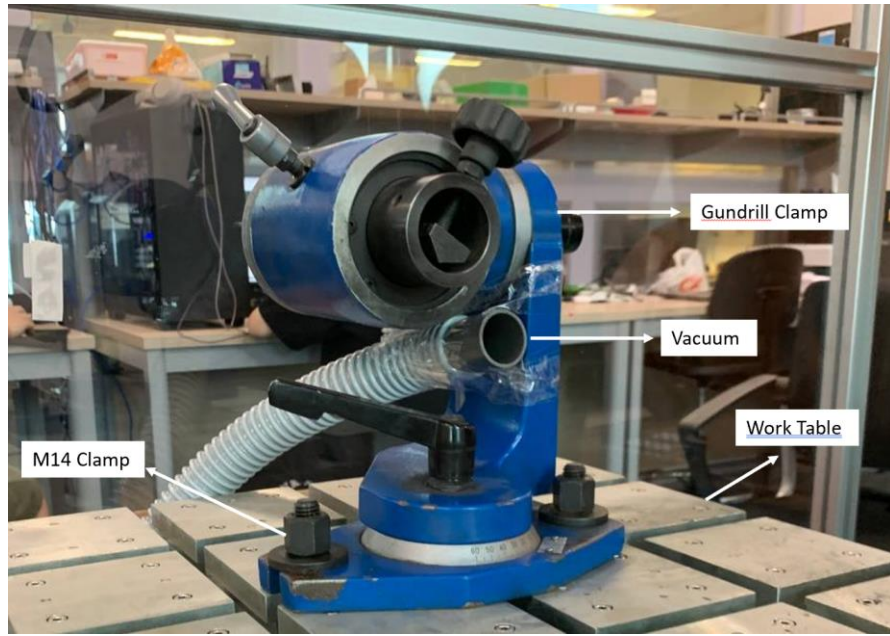


Figure 58: Gundrill Clamp Set-Up

The complete assembly for the testing procedure is illustrated in Figure 59 below. The gundrill clamp that holds the gundrill was clamped onto the worktable using a set of screw clamps from the M14 clamping kit. The team assessed the potential risks of the testing procedure, and the workspace was kept as tidy and organized as possible, to prevent any trips and falls.

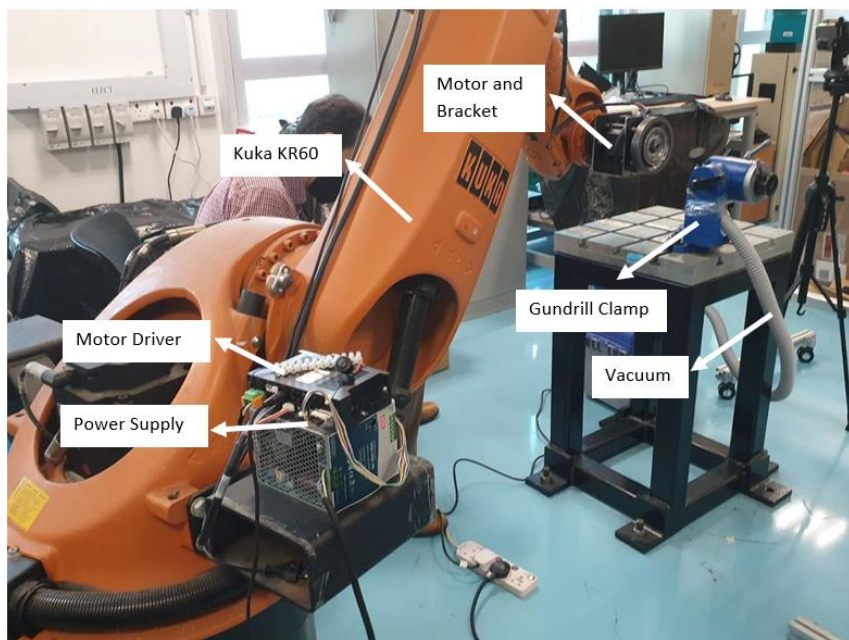


Figure 59: Full Assembly for Testing

9.4 Translation of Angles

In the current manual regrinding procedure, the angles on the gundrill clamp are adjusted to achieve grinding on certain spots of the gundrill at different orientations. However, since the automated solution is designed such that, the robotic arm will be doing most of the movement and rotation, the angles should be adjusted and translated onto the robotic arm. This section shows a pictorial representation of how the robotic arm will move, with respect to the gundrill clamp.

Translation of tilt angle

The figure below illustrates the tilt movement of the gundrill clamp in the manual regrinding procedure, from the side view. The gundrill tilts upwards at an angle of 20° while the robotic arm holding the grinding wheel does not tilt.

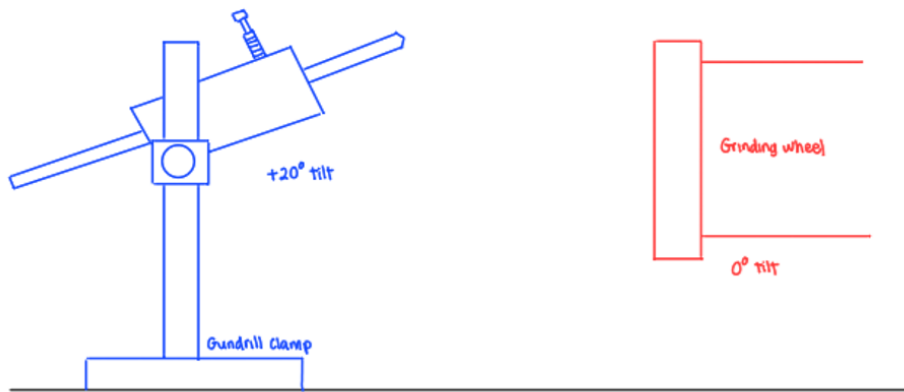


Figure 60: Tilt on Gundril Clamp (Original)

Conversely, the figure below illustrates the tilt movement of the robotic arm holding the grinding wheel, in the automated procedure, from the side view. The robotic arm tilts upwards at an angle of 20° while the gundrill clamp does not tilt.

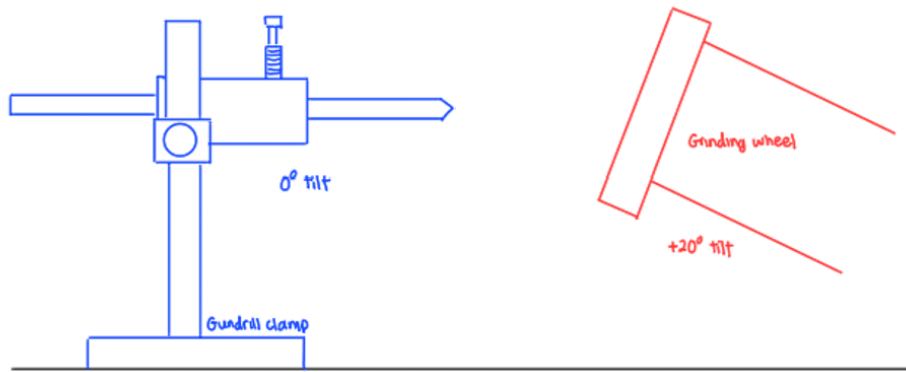


Figure 61: Tilt on Grinding Wheel (Translated)

Translation of swing angle

The figure below illustrates the swing movement of the gundrill clamp in the manual regrinding procedure, from the top view. The gundrill swings clockwise at an angle of 30° while the robotic arm holding the grinding wheel does not swing.

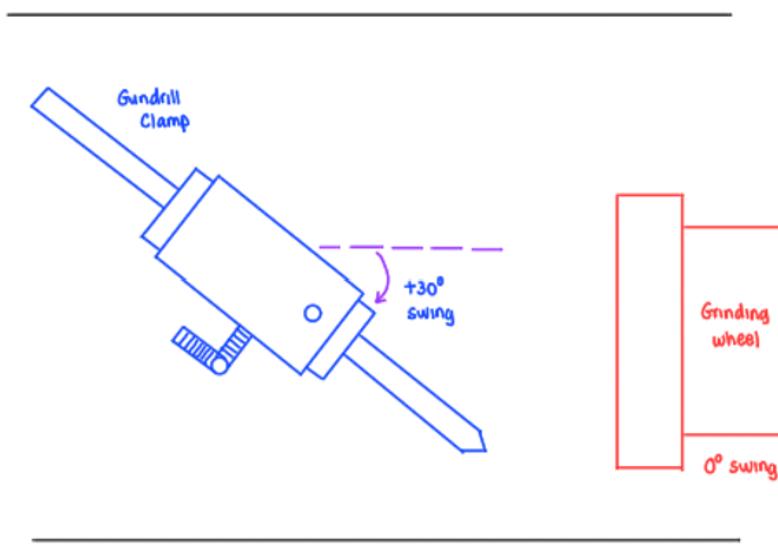


Figure 62: Swing on Gundrill Clamp

Conversely, the figure below illustrates the swing movement of the robotic arm holding the grinding wheel, in the automated procedure, from the top view. The robotic arm swings anti-clockwise at an angle of 30° while the gundrill clamp does not swing.

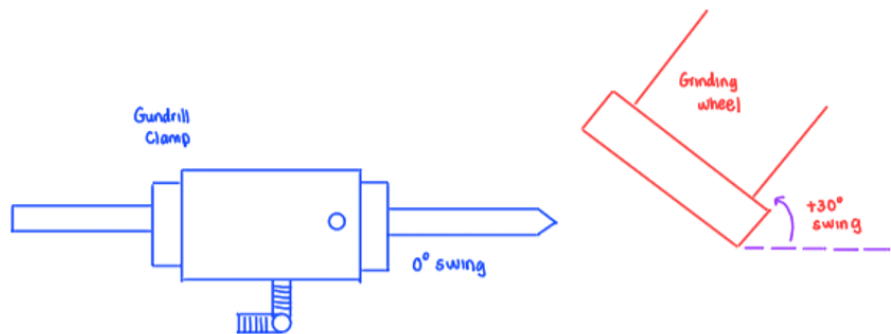


Figure 63: Swing on Grinding Wheel

Translation of torsion angle

For the automated procedure, the method of adjusting the torsion angle is the same as that for the manual regrinding procedure. Both procedures involve adjusting the torsion angle on the gundrill clamp itself. Therefore, there is no translation of torsion angle onto the robotic arm, in the automated procedure.

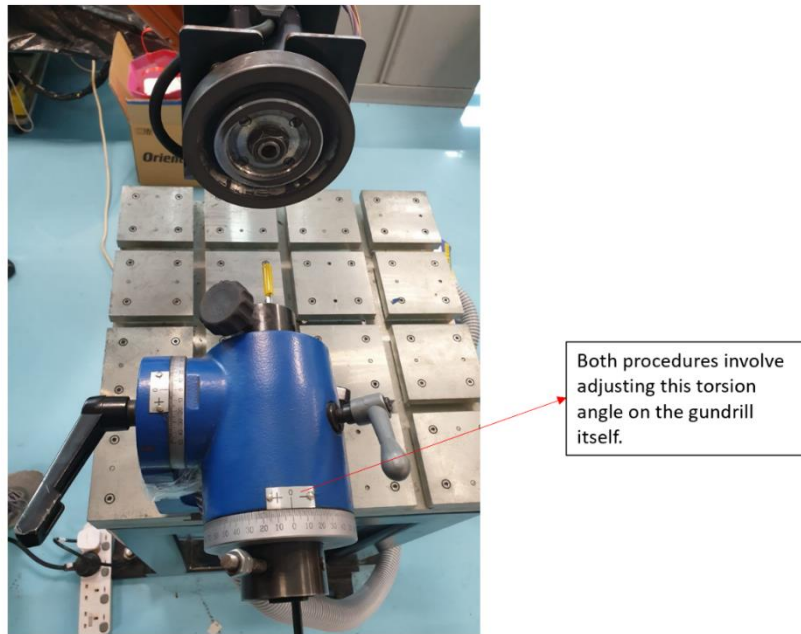
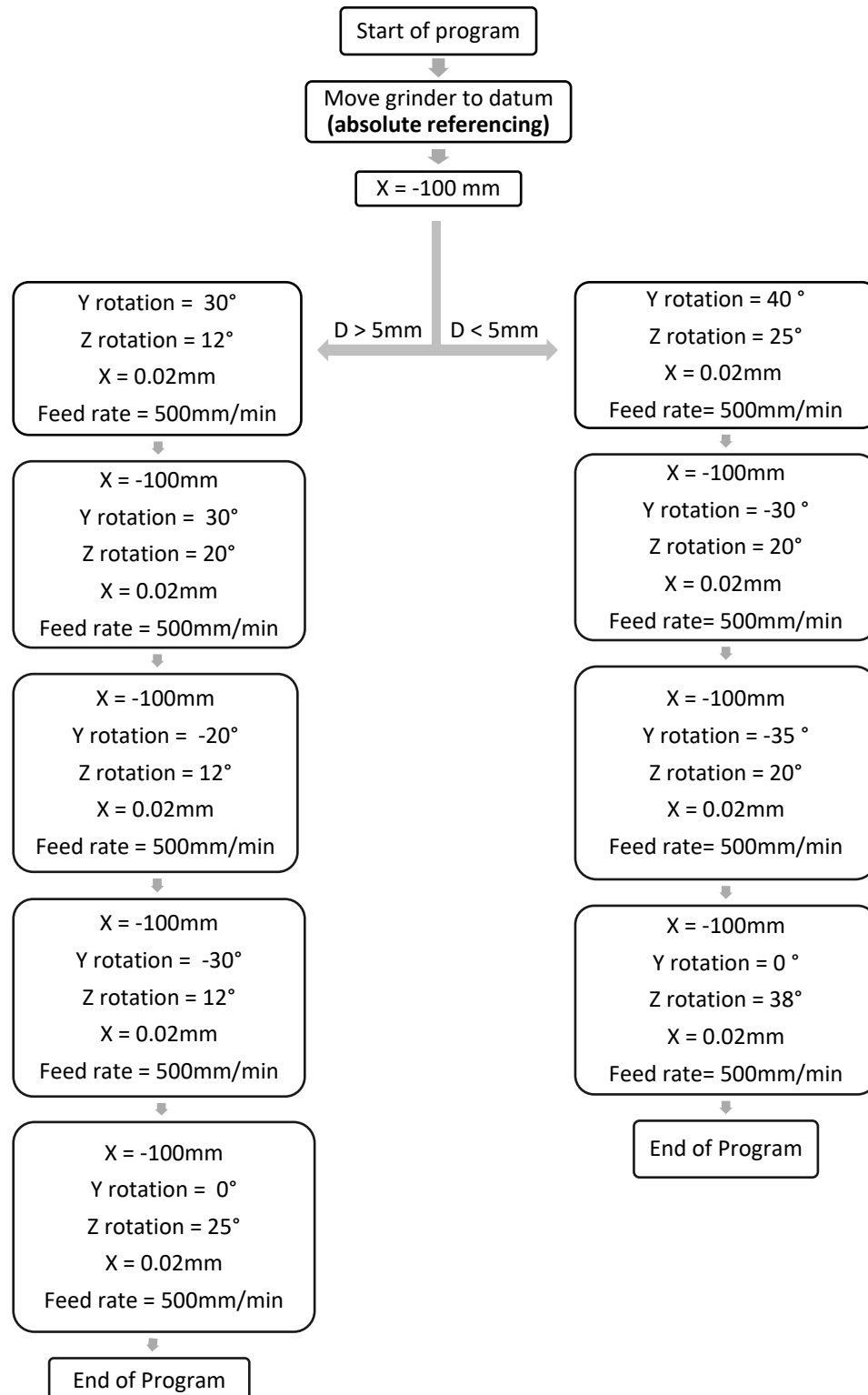


Figure 64: Torsion on Gundrill Clamp

9.5 Program Flow



The program flow as shown above describes the order in which the lines of codes for the robotic arm were executed. For testing, only the program for $D > 5\text{mm}$ (Diameter of gundrill exceeding 5mm) was carried out. With reference to Figure 7, the regrinding procedure chart, there are a total of six steps in the regrinding process, each with its own set of specific angles to be adjusted on the gundrill clamp. The final step (Step 6 in Figure 7 chart) was excluded from the program flow as it was rarely performed in the current manual regrinding process. Furthermore, for the testing, all the swinging (y rotation) and tilting motions (z rotation) were translated onto the grinding wheel. As a result, the positive and negative swinging angles (y rotation) were flipped, with respect to the robotic arm's plane of reference, while the tilting angles for the robotic arm remained the same (same sign). The depth of cut was then set to be 0.02mm and is repeated for 25 times at a feed rate of 500mm/min. The purpose of this was to obtain a total depth of cut of 0.5mm.

9.6 Testing Criteria

9.6.1 Dimensional Accuracy

Dimensional accuracy is one of the main points targeted by the problem statement. As mentioned in section 1.2, $\frac{1}{4}$ diameter is a very crucial dimension on the gundrill. Inaccuracy in this dimension can cause taper in the drilled hole, leading to failure. Therefore, $\frac{1}{4}$ diameter is used to define dimensional accuracy during the testing. Measurements of $\frac{1}{4}$ diameter of gundrills regrinded manually (initial $\frac{1}{4}$ diameter) were taken and recorded down before conducting the experiment. Once the experiment was completed, $\frac{1}{4}$ diameter was measured and recorded down again for comparison with the initial $\frac{1}{4}$ diameter. The experiment was carried out three times for better reliability. The design concept is proven to be successful if experimental $\frac{1}{4}$ diameter has lesser deviation from theoretical $\frac{1}{4}$ diameter compared to initial $\frac{1}{4}$ diameter.

9.6.2 Time Taken

Another point targeted by the problem statement is time taken for the regrinding process. The team's design aims to reduce the time taken for the regrinding process. According to the statistics that the team obtained from Halliburton, the manual regrinding process takes an average duration of 15 minutes, hence the benchmark used during the experiment is likewise 15 minutes.

Similarly, time was recorded during the three experiment trials. Design concept is proven to be successful if time taken for the experiment is less than 15 minutes.

9.7 Troubleshooting

This section describes some of the problems that the team has encountered during the experiment and how the team solved them.

9.7.1 Reference Axis

Initially, the team calibrated the robotic arm to be programmed based on a reference axis that was located on the face of the grinding wheel. As the team worked through the program, it was realised that having a reference axis on the wheel would affect the angles in the program flow. The angles in the program flow takes reference to an axis that is fixed. However, having the reference axis located on the wheel would also cause the axis to rotate as the robotic arm rotates according to the program flow. This would affect the subsequent angles that the robotic arm had to move to, causing unnecessary complication during the programming.

To resolve this issue, the team decided to re-calibrate the reference axis of the robotic arm to be located at the tip of the gundrill instead. This would allow the team to continue the experiment with the angles in the program flow and remove complications in the angles.

9.7.2 Reference Point

After calibration of the reference axis, a reference point must be set to define the point for grinding to begin, which is also the first point of contact between the grinding wheel and the gundrill. This reference point is also used to position the gundrill at the start of the experiment. A gundrill will be clamped down to have the tip touch the grinding wheel. This would aid in the programming of the depth of cut. A single reference point was set initially, however after running the program once through, little to no grinding was done in the fourth and final step of the program flow. The team realised that the reason was because the point of contact for each step was slightly different due to the angle of the grinding wheel. This caused inaccuracies in the actual depth of cut.



Figure 65: Calibration with Paper

To resolve this problem, reference points were manually set for each individual step, from steps 1 to 5. When setting the reference points, a piece of paper was used to ensure better accuracy. The paper was moved back and forth between the gundrill and grinding wheel while moving the grinding wheel towards the gundrill. Once the paper could no longer be moved and was suspended in the air, this indicated that there was contact between the gundrill and grinding wheel. To further improve the accuracy, the paper was removed, and the wheel was rotated. Contact between the gundrill and grinding wheel was indicated when there was friction (which generated a sound). These steps were utilised to ensure that there was enough contact between the gundrill and the grinding wheel.

9.7.3 Parallelism of grinding wheel

Inaccuracy in the parallelism of the grinding wheel can impact the accuracy of the grinding process. To check for parallelism, the tip of the gundrill was used as a reference. The x-axis distance of four points (top, bottom, left and right) on the grinding wheel must be equal to confirm parallelism of the grinding wheel. The grinding wheel was found to be unparallel and some possible reasons for it could be 1. Wear of grinding wheel. 2. Manufacturing defect of grinding wheel 3. Inaccuracy of manufactured motor bracket. To correct this, calibration had to be performed. Calibration was done by finding the highest point on the grinding wheel. The

highest point refers to the point where the grinding wheel sticks out of its plane the most. This highest point was then used as the reference point for the grinding.



Figure 66: Checking for Parallelism

9.8 Results

Measurements of the results of $\frac{1}{4}$ diameter were taken using the Keyence Microscope located at the Advanced Manufacturing Lab (AML). The diameter of the gundrill which used for testing was 6.35mm. Hence, the theoretical $\frac{1}{4}$ diameter of the gundrill was 1.5875mm. Accuracy of regrind is dictated by the closeness of the experimental $\frac{1}{4}$ diameter value to the theoretical $\frac{1}{4}$ diameter (1.5875mm).

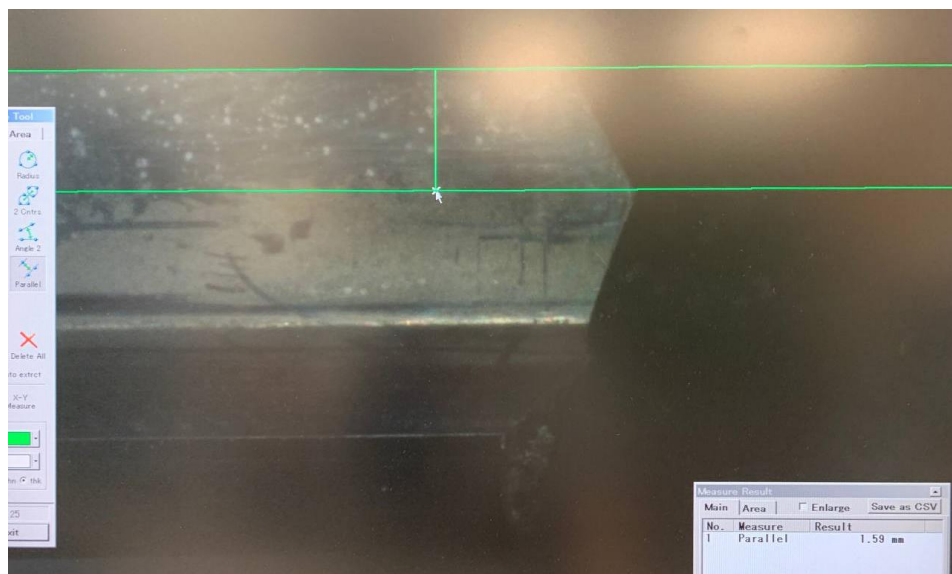


Figure 67: Display on Keyence Microscope

Table 11: Measurement of Three Gundrills (in mm) that were manually re-grinded at Halliburton

	First Reading	Second Reading	Third Reading	Average	Inaccuracy (Absolute value)
Gundrill 1	1.62	1.64	1.62	1.6267	0.0392
Gundrill 2	1.64	1.65	1.65	1.6467	0.0592
Gundrill 3	1.65	1.64	1.66	1.65	0.0625
Average Inaccuracy					0.0536

Table 12: Measurements of the Gundrill (in mm) re-grinded by the KR60

	First Reading	Second Reading	Third Reading	Average	Inaccuracy (Absolute value)
Trial Test 1	1.57	1.58	1.57	1.5733	0.0142
Trial Test 2	1.60	1.58	1.59	1.59	0.0025
Trial Test 3	1.61	1.63	1.63	1.6233	0.0358
Average Inaccuracy					0.0175

Table 13: Recorded Time Taken for each trial done on the KR60

Time taken for testing	
Trial Test 1	6 min 20 sec
Trial Test 2	6 min 08 sec
Trial Test 3	6 min 11 sec
Average Time Taken	6 min 13 sec

10. Discussion

10.1 Evaluation of Results

From the comparison of the results in Table 1111 and Table 1212, the average inaccuracy for gundrills re-grinded on the KR60, 0.0175 mm, is significantly lower than that of the manually re-grinded gundrills, 0.0536 mm. Therefore, there was an improvement in accuracy of 0.0361 mm (67% improvement from 0.0536 mm inaccuracy from manual regrind). However, it can be observed that the average $\frac{1}{4}$ diameter values of the gundrills shows an increasing trend as more trials are performed. The team concluded that the reason for the poor results in trial 3 is due to calibration and the reference gundrill used. Calibration is done by taking reference of the gundrill, hence inaccuracy in the reference gundrill can cause deviation in the end results of the grinding. As more trials are performed, the inaccuracy builds up and causes the overall accuracy to drop. Accuracy in the reference gundrill is crucial in determining the accuracy of the automated grinding.

In the experiment conducted, the system is not fully automated yet, hence the time recorded includes the time taken for the grinding process as well as the time needed for manual rotation of the x-axis. Even so, the average time taken for each trial is 6 minutes and 13 seconds, which is still much faster than the manual regrinding procedure (10 to 15 minutes). Therefore, there was a decrease in grinding time by 8 minutes 47 seconds (59% improvement from 15 minutes by manual regrinding). Results of time required for the grinding process are expected to be further reduced with the fully automated system (with the implementation of the torque motor). As the project was still in the experimental phase, robotic arm movements (except for feed rate) were slowed down for safety purposes, but during the actual implementation, robotic arm movements can be sped up to improve the time needed for grinding. Having the process automated also brings about more benefits as technicians can be freed up during this automated process.

Results from the experiment conducted were satisfactory, in comparison to the current method used at Halliburton. Considering the multitude of factors, it can be concluded that the design to automate the process is successful.

10.2 Limitations of Design

Due to the design of the grinding wheel, the automated design is only suitable for gundrills of diameter smaller than the width of the diamond band on the wheel, 15.06mm. For gundrills with diameters larger than the band, dimensional accuracy will be compromised as grinding around the edges of the gundrill which exceeds the band will not take place.



Figure 68: Width of Diamond Band

Another limitation to the design concept is the initial calibration. To ensure accuracy of the regrinding, gundrills of different diameter must be calibrated once. This can be an exhausting procedure due to the wide range of gundrill sizes at Halliburton as well as the taxing process of calibration.

In addition, the programming software for the KR60 may not be as user-friendly and flexible when making minor changes to the program. To modify the program, recalibration for each step is required. The software does not allow the user to select a certain step in the program to be executed. Hence, to carry out a specific step, the program must start from the beginning. This

causes the depth of cut to vary for each step of the regrinding process, with the first few cuts being deeper than the subsequent cuts. Therefore, the accuracy of the dimensions is compromised.

10.3 Recommendations

Based on the limitations observed by the team, it is possible to improve the current set-up with several changes. The following are the viable solutions to target the limitations of the grinding wheel design:

- Changing the grinding wheel design by increasing diamond band width
- Programming robotic arm to translate left and right in the z-axis so that gundrill surfaces can be evenly grinded even when diameter is greater than band width.

The design can be further refined by installing sensors on the robotic arm to improve the accuracy in calibration and speed up the calibration process. This will also help in increasing the accuracy of the regrinding process as it gives feedback to the system. However, this would mean that the costs will increase significantly.

It is also recommended to use a gundrill that is as close to the ideal dimensions as the “Golden Standard” during calibration. This ‘Golden Standard’ refers to the gundrill with the ideal dimensions and angles grinded off its tip. This will ensure that calibration is accurate and results from grinding will be optimal.

11. Conclusion

The automated regrinding system can perform the process of regrinding of carbide tip of gundrills safely, efficiently, and accurately. Through the results from the simulation and testing, the automated regrinding system can withstand the estimated grinding loads and the high stress conditions.

Experimental results have shown an improvement in accuracy of 0.0361 mm (67% improvement from 0.0536 mm inaccuracy from manual reground) and a decrease in grinding time by 8 minutes 47 seconds (59% improvement from 15 minutes by manual regrinding). Based on the results obtained, the design concept is proven to be successful. Despite the benefits that the design

concept brings about, there are several limitations to it. The grinding wheel design only allows regrinding of gun-drills smaller than the width of its diamond band and the initial calibrations can be tedious and time-consuming.

Although initial calibrations are laborious, the end results of the experiment demonstrated increased accuracy and improved grinding time. With an estimated cost of approximately SGD\$50,000, the team believes that the expensive cost is reasonable, based on the efficiency of the design concept and the satisfactory results.

The design concept can be further improved by exploring the effectiveness through adding various sensors, such as force sensors, to help with the accuracy and the programming process. Design of the grinding wheel or programming of the robotic arm can also be modified to suit a wider range of gun-drill diameters.

12. References

- [1] Halliburton Company, “About Us,” Halliburton Company, [Online]. Available: <https://www.halliburton.com/en/about-us>. [Accessed 23 October 2021].
- [2] Singapore Economic Development Board, “Halliburton,” Singapore Economic Development Board, 11 June 2021. [Online]. Available: <https://www.edb.gov.sg/en/our-industries/company-highlights/halliburton.html>. [Accessed 23 October 2021].
- [3] R. S. Woodbury, History of the Grinding Machine, Cambridge: Technology Press, 1959.
- [4] W. B. Rowe, Principles of Modern Grinding Technology (2nd ed), Oxford: Elsevier Inc., 2014.
- [5] F. Klocke, E. Brinksmeier and K. Weinert, “Capability Profile of Hard Cutting and Grinding Processes,” *CIRP Annals*, vol. 54, no. 2, pp. 557-58, 2005.
- [6] I. Inasaki, H. Tönshoff and T. Howes, “Abrasive Machining in the Future,” *CIRP Annals*, vol. 42, no. 2, pp. 723-732, 1993.
- [7] Amon Engineering, “A Quick Guide to Surface and Cylindrical Grinding,” Amon Engineering, 7 April 2020. [Online]. Available: <https://www.amonengineering.com.au/a-quick-guide-to-surface-and-cylindrical-grinding/>. [Accessed 26 October 2021].
- [8] UNISIG, “What is Gundrilling?,” UNISIG, [Online]. Available: <https://unisig.com/information-and-resources/what-is-deep-hole-drilling/what-is-gundrilling/>. [Accessed 2 November 2021].
- [9] Triumph Tool, “Advantages of Gundrilling for Deep Hole Drilling,” Triumph Tool, 21 November 2019. [Online]. Available: <https://www.triumphtool.com/metal-working-tools-blog/advantages-of-gundrilling/>. [Accessed 2 November 2021].
- [10] D. W. K. Neo, A. S. Kumar and M. T. Lew, “Chapter 3 - Gun drilling of difficult-to-machine materials,” *Advanced Machining and Finishing*, pp. 77-141, 2021.
- [11] E. Krueger and R. Funk, “Time to Rethink Resharpening Gundrills,” UNISIG, 1 April 2019. [Online]. Available: <https://unisig.com/time-to-rethink-resharpening-gundrills/>. [Accessed 2 November 2021].
- [12] Profidrill, “The Effects of Tool Degradation on Hole Straightness in Deep Hole Gundrilling,” Profidrill, [Online]. Available: <https://www.deepholemachines.com/boringbars-drillgrinders-accesoiries-options/gun-drill-grinding-machine-gun-drill-sharpening-machine-resharpening-machine>. [Accessed 2 November 2021].

- [13] Carbide Processors Inc, “Grinding Carbide- Health and safety risks,” Carbide Processors Inc, [Online]. Available: <https://carbideprocessors.com/pages/technical-info/grinding-carbide-health-and-safety-risks.html>. [Accessed 1 November 2021].
- [14] “Blog,” CCM, January 2019. [Online]. Available: <https://www.ccmrails.com/2019/01/17/what-is-a-linear-module/>. [Accessed 8 November 2021].
- [15] Robbie Dickson, “Linear Actuators 101,” Firgelli Automations, 16 November 2018. [Online]. Available: <https://www.firgelliauto.com/blogs/news/linear-actuators-101>. [Accessed 8 November 2021].
- [16] A. Joubair, “What are Accuracy and Repeatability in Industrial Robots?,” RoboticQ, 7 October 2014. [Online]. Available: <https://blog.robotiq.com/what-are-accuracy-and-repeatability-in-industrial-robots>. [Accessed 3 March 2022].